New Phytologist

Research

Zymoseptoria tritici stealth infection is facilitated by stage-specific downregulation of a β-glucanase

Diego Rebaque[1,2,3]*, Cristian Carrasco-López[1]*, Parvathy Krishnan[4], Gemma López[1], Sergio López-Cobos[1], Felipe de Salas[5], Lukas Meile[1], Cécile Lorrain[4], Asier Largo-Gosens[3], Bruce A. McDonald[4], Francisco Vilaplana[2], María Jesús Martínez[5], Hugo Mélida[3,6], Antonio Molina[1,7] and Andrea Sánchez-Vallet[1]

[1]Centro de Biotecnología y Genómica de Plantas, Universidad Politécnica de Madrid (UPM) – Instituto Nacional de Investigación y Tecnología Agraria y Alimentaria (INIA/CSIC), Campus de Montegancedo UPM, 28223, Pozuelo de Alarcón, Madrid, Spain; [2]Division of Glycoscience, Department of Chemistry, School of Engineering Sciences in Chemistry, KTH Royal Institute of Technology, 11428, Stockholm, Sweden; [3]Área de Fisiología Vegetal, Departamento de Ingeniería y Ciencias Agrarias, Universidad de León, 24071, León, Spain; [4]Plant Pathology, Institute of Integrative Biology, ETH Zürich, 8092, Zürich, Switzerland; [5]Centro de Investigaciones Biológicas Margarita Salas, Spanish National Research Council, C/ Ramiro de Maeztu 9, 28040, Madrid, Spain; [6]Instituto de Biología Molecular, Genómica y Proteómica (INBIOMIC), Universidad de León, 24071, León, Spain; [7]Departamento de Biotecnología-Biología Vegetal, Escuela Técnica Superior de Ingeniería Agronómica, Alimentaría y de Biosistemas, UPM, 28040, Madrid, Spain

Authors for correspondence:
Andrea Sánchez-Vallet
Email: andrea.sanchezv@upm.es

Antonio Molina
Email: antonio.molina@upm.es

Received: *27 June 2025*
Accepted: *9 September 2025*

New Phytologist (2025) **248:** 3191–3207
doi: 10.1111/nph.70621

Key words: damage-associated molecular pattern, pathogen effector, plant cell wall, plant resistance, *Triticum aestivum*, wheat immunity, *Zymoseptoria tritici*, β-1,3/1,4-mixed-linked glucans.

Summary

- Plant cell walls constitute a major defence barrier against pathogens, although it is unclear how specific cell wall components impact pathogen colonisation. Pathogens secrete cell wall-degrading enzymes (CWDEs) to facilitate plant colonisation, but damaged or infected cells are often a source of cell wall-derived oligosaccharides that trigger host immunity. The mechanisms by which pathogens minimise the release of cell wall-derived oligosaccharides while colonising the host remain to be elucidated.
- We combined biochemical, molecular, and transcriptomic analyses to functionally characterise a glycoside hydrolase (*Zt*GH45) from the wheat pathogen *Zymoseptoria tritici*.
- *ZtGH45* gene is expressed during the necrotrophic phase. At this stage, wheat β-1,3/1,4-mixed-linked glucan (MLG)-derived oligosaccharides are also accumulated. We show that overexpression of *ZtGH45* in *Z. tritici* enhances hydrolysis of MLG from wheat cell walls, and the released MLG oligosaccharides trigger an immune response in wheat. The results demonstrate that tight regulation of *ZtGH45* is critical for the infection process as it prevents early accumulation of MLG oligosaccharides that would prematurely induce host immunity, thereby counterbalancing fungal virulence.
- We suggest that the balance between plant cell wall degradation by fungal CWDEs and the release of immunogenic wall-derived oligosaccharides governs the outcome of host invasion by pathogens.

Introduction

Successful plant colonisation largely depends on the pathogen's ability to overcome the host resistance machinery and efficiently acquire nutrients (Haueisen & Stukenbrock, 2016). Plant cell walls act not only as defensive barriers against potential pathogens but also as a source of nutrients and biosynthetic building blocks for colonising microorganisms. To surmount this defensive barrier and acquire plant nutrients, fungal pathogens secrete an arsenal of cell wall-degrading enzymes (CWDEs). CWDEs are a subset of carbohydrate-active enzymes (CAZymes, Drula *et al.*, 2022), such as glycoside hydrolases (GHs), which hydrolyse the glycosidic linkage of carbohydrates present in plant cell walls. The activity of CAZymes on wall polysaccharides can lead to the release of plant cell wall-derived glycans, which can function as elicitors of host immune responses and are commonly known as damage-associated molecular patterns (DAMPs; Molina *et al.*, 2024a,b).

Plant cell wall-derived glycans can be perceived by plant pattern recognition receptors (PRRs), triggering a cascade of defence responses referred to as pattern-triggered immunity (PTI) that include the accumulation of reactive oxygen species (ROS), stomatal closure, callose accumulation, and upregulation of defensive genes (Bigeard *et al.*, 2015; Boutrot & Zipfel, 2017; Gust *et al.*, 2017; Bacete *et al.*, 2018; Molina *et al.*, 2024b). Thoroughly investigated plant cell wall-derived oligosaccharides acting as DAMPs include oligogalacturonides derived from pectins (Hahn *et al.*, 1981; Voxeur *et al.*, 2019), as well as

*These authors contributed equally to this work.

oligosaccharides derived from xyloglucans (Claverie *et al.*, 2018), mannans (Zang *et al.*, 2019), callose (Mélida *et al.*, 2018), arabinoxylan (Mélida *et al.*, 2020), xylans (Pring *et al.*, 2023; Ferná ndez-Calvo *et al.*, 2024), cellulose (Aziz *et al.*, 2007; Martín-Dacal *et al.*, 2023), and β-1,3/1,4-glucan (Rebaque *et al.*, 2021; Yang *et al.*, 2021). β-1,3/1,4-glucans, also known as mixed-linked glucans (MLGs), consist of linear polymers of glucose molecules linked by β-1,4 and β-1,3 bonds and are a distinctive feature of the plant cell walls of Equisetaceae and *Poaceae* species (Labavitch & Ray, 1978; Fry *et al.*, 2008; Sørensen *et al.*, 2008; Fuertes-Rabanal *et al.*, 2025). MLG oligosaccharides can also be derived from the walls of oomycetes and be perceived by the host as microbe-associated molecular patterns (MAMPs), triggering PTI (Rebaque *et al.*, 2021). Regardless of their origin, MLG-derived oligosaccharides, particularly the well-characterised trisaccharide β-D-cellobiosyl-1,3-β-D-glucose (MLG43), confer enhanced disease resistance to pathogens in several plant species, including Arabidopsis, tomato, pepper, barley, and rice (Barghahn *et al.*, 2021; Rebaque *et al.*, 2021; Yang *et al.*, 2021). Recent works have shown that the LysM receptor kinase Chitin Elicitor Receptor Kinase 1 (CERK1) and Lectin Receptor Kinase 1 (LecRK1) are involved in the perception of MLG oligosaccharides in rice (Yang *et al.*, 2021; Dai *et al.*, 2023). In Arabidopsis, Leucine-Rich Repeat-Malectin Receptor Kinases (LRR-MAL RKs), Impaired in Glycans Perception 1 (IGP1/CORK1), IGP3 and IGP4, and the LysM-containing receptors CERK1, LYK4, and LYK5 are required for the perception of MLG oligosaccharides (Rebaque *et al.*, 2021; Martín-Dacal *et al.*, 2023).

Septoria tritici blotch is one of the major diseases of wheat globally and is caused by the fungal pathogen *Zymoseptoria tritici* (Meile *et al.*, 2025). This fungus harbours in its genome 203 genes encoding putative glycoside hydrolases (GHs), which potentially function as CWDEs (Drula *et al.*, 2022). The initiation of the infection cycle in *Z. tritici* occurs upon the germination of either a sexual or an asexual spore on the surface of plant leaves. Following stomatal penetration, the fungus colonises the apoplastic space in intimate interaction with plant cell walls without exhibiting any visible signs of plant damage. This asymptomatic phase can last several days (8–20 d) depending on the wheat genotype, the *Z. tritici* strain, and the environmental conditions. After this phase, the pathogen produces chlorotic lesions that will subsequently become necrotic and initiates the necrotrophic phase (Kema *et al.*, 1996; Duncan & Howard, 2000; Keon *et al.*, 2007; Deller *et al.*, 2011; Sánchez-Vallet *et al.*, 2015; Steinberg, 2015). Effector recognition by wheat resistant cultivars prevents *Z. tritici* penetration through the stomata and the subsequent apoplast colonisation (Battache *et al.*, 2022, 2024; Alassimone *et al.*, 2024). At the onset of necrotic symptoms, fungal growth spikes and the reproductive structures, known as pycnidia and pycnidiospores, are produced (Steinberg, 2015). Distinct sets of virulence factors are postulated to be required throughout the different phases of a *Z. tritici* infection. In fact, several predicted cellulases, hemicellulases, pectinases, and cutinases show a specific life-cycle-dependent expression pattern during wheat infection (Brunner *et al.*, 2013; Palma-Guerrero *et al.*, 2017). However, the mechanistic contribution of CWDEs to *Z. tritici* virulence remains largely unknown. In other pathogens, several CWDEs have been shown to play key roles in the infection process through diverse mechanisms, such as nutrition or hydrolysis of immunity-triggering elicitors (Esquerré-Tugayé *et al.*, 2000; Bradley *et al.*, 2022). Impairment of the cellulose degradation machinery in the soil-borne fungus *Fusarium oxysporum* increases its virulence in Arabidopsis (Gámez-Arjona *et al.*, 2022). Moreover, constitutive expression of two endoglucanases from the GH12 family (*MoCel12A* and *MoCel12B*) in the rice pathogen *Magnaporthe oryzae* results in an increased release of MLG-derived DAMPs and a reduction of symptom development (Yang *et al.*, 2021). These findings indicate that the activity of CWDEs may also lead to the release of oligosaccharides that act as DAMPs, thereby activating plant immune responses and potentially limiting infection (Yang *et al.*, 2021; Molina *et al.*, 2024b).

In this study, we identified a GH belonging to the GH45 family from *Z. tritici* (*ZtGH45*) and demonstrated that its expression is tightly regulated, occurring only during the necrotrophic phase of the fungus. Overexpression of *ZtGH45* in *Z. tritici* leads to a reduced fungal virulence and an enhanced release of MLG-derived oligosaccharides. Such MLG oligosaccharides trigger disease resistance responses in wheat, which involve ROS accumulation, stomatal closure, and transcriptional activation of defensive genes, and hinder *Z. tritici* infection progression. We propose that tuning the expression of CWDEs, such as *ZtGH45*, impacts pathogen colonisation and host recognition.

Materials and Methods

Growth conditions for *Zymoseptoria tritici* and bacterial strains

The Swiss *Zymoseptoria tritici* (Desm.). strain ST99CH_3D7 (abbreviated as 3D7; Linde *et al.*, 2002) was used in this study. *Zymoseptoria tritici* was grown in yeast sucrose broth (YSB, 1% w/v yeast extract and 1% w/v sucrose) or in yeast peptone dextrose (YPD, 1% w/v yeast extract, 2% w/v peptone, and 2% w/v dextrose) amended with 50 μg ml^{-1} kanamycin sulphate, at 18°C, 120 rpm in 100-ml Erlenmeyer flasks. Blastospores from *Z. tritici* were collected after 6 d and used for the infection and developmental assays. Liquid fungal cultures were filtered through double-layered sterile cheesecloth, blastospores were collected by centrifugation at 3273 ***g*** for 15 min at 4°C and resuspended in water. Blastospore concentration in the suspension was determined using Neubauer counting chambers. For molecular cloning and plasmid propagation, *Escherichia coli* strain NEB® 5-alpha (New England Biolabs, Ipswich, MA, USA) and Stellar™ Competent Cells (TaKaRa Bio Inc., Shiga, Japan) were used. *Escherichia coli* was grown on LB media (1.6% w/v tryptone, 1% w/v yeast extract, 0.5% w/v NaCl) amended with kanamycin sulfate (50 μg ml^{-1}) at 37°C. *Agrobacterium tumefaciens* strain AGL1 was grown at 28°C in LB media containing kanamycin sulfate (50 μg ml^{-1}), carbenicillin (100 μg ml^{-1}), and rifampicin (50 μg ml^{-1}), and used for *Agrobacterium*-mediated transformation of *Z. tritici*.

Generation of *Z. tritici* transformants

Based on RNA-seq reads (NCBI accessions: SRA SRP152081 and SRP077418), we amended the annotation of the *ZtGH45* gene in the 3D7 genome. For the strains 3D1 and 1E4, the gene was correctly annotated. We obtained two types of overexpression lines, one in which the gene was inserted *in locus* and the second one with the ectopic insertion. To obtain *Z. tritici* lines overexpressing *ZtGH45* (*ZT3D7_G10118*, *ZtIPO323_110030*, *Zt09_chr_10_00532*, *Mycgr3_76589*; *ZtGH45_OE*, Supporting Information Table S1) *in locus*, the *Aspergillus nidulans* glyceraldehyde-3-phosphate dehydrogenase (*gpdA*) promoter was inserted upstream of the start codon of *ZtGH45* by homologous recombination in the strain 3D7. Up- and downflanking regions (*c.* 1000 bp) were amplified from 3D7 genomic DNA using PfuTurbo® Cx Hotstart DNA polymerase (Stratagene, Cedar Creek, TX, USA). USER Friendly cloning technique was used to fuse the flanking regions to the binary vector backbone of prfHU2E (Frandsen *et al.*, 2008). Fusion was performed using USER enzyme mix from New England Biolabs and the plasmid (Fig. S1a) was cloned in *E. coli*, following the manufacturer's instructions. To obtain *Z. tritici* lines ectopically overexpressing the wild-type (WT) or mutated version of *ZtGH45* generated either with or without a C-terminal 3× HA epitope tag (ZtGH45_OE^{WT}, ZtGH45_OE$^{D37A/D145A}$, ZtGH45_OE$^{WT\text{-}3xHA}$, and ZtGH45_OE$^{D37A/D145A\text{-}3xHA}$), the plasmids were assembled using the In-Fusion HD Cloning Kit (TaKaRa Bio Inc.). Previously, the pCCL1 plasmid was constructed by inserting the *gpdI* promoter upstream of the *Ttef* terminator into the pLM1 plasmid (Fig. S1b,c; Meile *et al.*, 2020). The WT PCR product of *ZtGH45* (from start to stop codons) was obtained from 3D7 genomic DNA and the catalytically dead version (D37A and D145A) was constructed by PCR-driven mutagenesis, as described (Heckman & Pease, 2007). The 3× HA coding fragment was amplified by PCR from the pGWB614 vector (Nakamura *et al.*, 2010). The corresponding fragments were inserted between the *gpdI* promoter and the *Ttef* terminator of the EcoRV-linearised pCCL1 plasmid. The plasmid used for targeted deletion of the *ZtGH45* gene via homologous recombination was constructed as previously described (Suarez-Fernandez *et al.*, 2023). Briefly, a PCR fragment containing the hygromycin resistance gene was flanked by *c.* 1.1 kb homology arms corresponding to the *ZtGH45* locus. This fragment was assembled into the KpnI- and SbfI-linearised pCGEN plasmid using the In-Fusion HD Cloning Kit (Takara Bio, Japan; Fig. S1d). All PCR amplifications were performed using Supreme NZYProof 2× Green Master Mix (NZYTech, Lisboa, Portugal), and the primers listed in Table S2. The *Z. tritici* overexpressing mutants were obtained by *A. tumefaciens*-mediated transformation and selected using hygromycin (100 μg ml^{-1}) as previously described (Zwiers & De Waard, 2001; Krishnan *et al.*, 2018; Meile *et al.*, 2020). *In locus* insertion of the overexpression mutant (*ZtGH45_OE*) was confirmed by PCR (Fig. S1e–f; primers in Table S2).

Zymoseptoria tritici infection assays

Wheat (*Triticum aestivum* L.) cultivars Titlis, Drifter, Fielder, and Paragon were grown in a growth chamber at 18°C during the day and 15°C during the night and 60% relative humidity for 15 d, as described (Suarez-Fernandez *et al.*, 2023). A suspension of 5 × 10^6 or 10^7 spores ml^{-1} of *Z. tritici* in water with 0.1% v/v Tween 20 was used to spray-inoculate wheat leaves (1 ml per plant). Upon infection, plants were placed in sealed plastic bags for 48 h to maintain high humidity. For the protection assay, 24 h before infection, wheat plants were sprayed (1 ml per plant) with a solution of 0.5 mM of β-D-cellobiosyl-1,3-β-D-glucose (MLG43; O-BGTRIB; Megazyme, Auchincruive, UK) or 0.5 mM cellotriose (Cello3; O-CTR; Megazyme) with the adjuvants UEP-100 (0.1% v/v; Croda, Snaith, UK) and Tween 20 (0.01% v/v). The adjuvant solution alone was used as the mock control. Disease symptoms in second leaves were estimated at 13–18 d post infection (dpi), as described by Meile *et al.* (2018). Leaves were analysed using ImageJ (Schneider *et al.*, 2012) and an automatic image analysis method (Stewart *et al.*, 2016) to estimate the percentage of leaf area covered by lesions and pycnidia density (pycnidia cm^{-2} of leaf or pycnidia cm^{-2} of lesion).

Zymoseptoria tritici developmental assay

A 3-μl drop at 10^6 spores ml^{-1} of each *Z. tritici* line was placed on solid YMS (0.4% w/v yeast extract, 0.4% w/v malt extract, 0.4% w/v sucrose, and 1.2% w/v Bacto™ Agar) amended with 1 mM H_2O_2, 1 M sorbitol, 0.5 M NaCl, or 200 ng μl^{-1} Calcofluor white or on Vogel's minimal media (Vogel, 1956) amended with 5 g l^{-1} sucrose, 5 g l^{-1} fructose, 5 g l^{-1} carboxymethyl cellulose (CMC) sodium salt (C4888; Sigma-Aldrich), or 5 g l^{-1} barley β-glucan (P-BGBL; Megazyme). Plates were incubated at 18°C, except for one of the plates that was incubated at 28°C, for 6 d.

In vitro assays of β-glucan enzymatic degradation

Zymoseptoria tritici and wheat alcohol insoluble residue (AIR) were obtained as described by Rebaque (2021) with modifications. *Zymoseptoria tritici* blastospores were grown in YPD media for 6 d as indicated above. After centrifugation at 3273 ***g*** for 15 min at 4°C, the cells were washed twice with distilled water. *Zymoseptoria tritici* cells and dry leaves of 17-d-old wheat plants were fine-powdered and washed three times with 30 ml g^{-1} methanol/chloroform (1 : 1; v/v), shaking at 4°C for 1 h, overnight, and 1 h, respectively. After each step, centrifugation at 3273 ***g*** for 10 min at 4°C was performed, and supernatants were discarded. Pellets were washed with acetone for 1 h, and the resulting pellet was dried. Samples were treated with 30 ml g^{-1} 70% v/v ethanol twice overnight and for 1 h. After this last treatment, pellets were washed with acetone, dried, and considered as AIR. For β-1,3-1,4-glucan quantification in wheat and *Z. tritici* AIR, the β-Glucan Assay Kit (Mixed Linkage; K-BGLU, Megazyme) was used.

To determine β-glucan oligosaccharides released by the *Z. tritici* lines (3D7-GFP, Δ*gh45*, ZtGH45_OE^{WT}, and ZtGH45_OE$^{D37A/D145A}$ for Fig. 2 (see later); and 3D7 and three independent lines of *in locus* ZtGH45_OE for Fig. S2 (see later)), a spore suspension of each line of *Z. tritici* at a concentration of 4×10^5 spores ml^{-1} was grown in Vogel's minimal medium (Vogel, 1956) with 0.5% (w/v) fructose as a carbon source to avoid the presence of free glucose in the media. For the β-1,3/1,4-glucan, cellulose, and AIR degradation assay, commercial barley β-glucan (P-BGBL; Megazyme), CMC sodium salt (C4888; Sigma-Aldrich), or wheat AIR were added to the media at a concentration of 0.5% (w/v). Cellulase (EC 3.2.1.4; endo-1,4-β-D-glucanase from *Aspergillus niger*; Megazyme) at 2.5 U ml^{-1} was used as a positive control. The released oligosaccharides were partially purified from the supernatant of 96-h-old cultures by adding one volume of 100% ethanol and precipitating the polymers at −20°C overnight (Voxeur *et al.*, 2019). Samples were centrifuged at 5000 ***g*** for 10 min at 4°C, and the supernatants were collected and freeze-dried. β-glucan oligosaccharides released in the media of four different biological replicates were quantified using the modified β-Glucan Assay Kit (Mixed Linkage; K-BGLU, Megazyme). Samples were directly treated with β-glucosidase following the protocol of the manufacturer. Serial D-glucose dilutions were used to perform the standard calibration curve. In addition, to identify the released oligosaccharides, samples from the commercial barley β-glucan were analysed with HPAEC-PAD in an LC 930 Compact IC Flex (Metrohm) chromatography system with an IC pulsed amperometric detector (FlexiPAD). Oligosaccharides were separated using a Metrosep Carb 2250/4.0 (Metrohm) analytical column and a Metrosep Carb 2 Guard/4.0 (Metrohm) guard column at 40°C with an isocratic 200 mM NaOH and 150 mM sodium acetate and variable flux: 0–12 min at 0.7 ml min^{-1}, 12.1–22.0 min at 0.9 ml min^{-1}, and 22.1–27.0 min at 0.7 ml min^{-1}. For oligosaccharide quantification, standard curves of D-glucose (PanReac), D-fructose (Merck), MLG43 (O-BGTRIB; Megazyme), Cello3 (O-CTR; Megazyme), and MLG443 (O-BGTETB; Megazyme) commercial standards were used. MLG4443, MLG_HDP1, and MLG_HDP2 were purified according to Rebaque *et al.* (2021). The experiment was performed two times independently.

Characterisation of *in planta* β-glucan oligosaccharide production

For the *in planta* identification and quantification of oligosaccharide production during the course of the infection, wheat plants were infected as described above using 3D7. Two centimetres from the second leaf tips were discarded, and the adjacent 13 cm from each leaf were collected and frozen in liquid nitrogen. Three independent biological replicates, each consisting of 2 second leaves per treatment, were collected for oligosaccharide analysis at 6, 8, and 10 dpi. Samples were homogenised in liquid nitrogen and freeze-dried. In this study, 10–15 mg of dry material was resuspended in 0.5 ml deionised water, ultrasonicated for 10 min, and heated at 95°C for 10 min. After cooldown, samples were centrifuged for 10 min at 17 000 ***g***. Supernatants were filtered through 10 kDa MWCO Centrifugal Filters (Amicon®, Ultracel®). A second extraction was performed using the same pellets following the same procedure, and both supernatants were pooled together. Oligosaccharide-containing filtered supernatants were freeze-dried and resuspended in 0.1% formic acid-acetonitrile (1 : 1 v/v). For HILIC-ESI-MS, samples were injected onto a XBridge Amide column (3.5 µm, 2.1 × 150 mm; Waters, Milford, MA, USA) with a flow of 0.8 ml min^{-1}. The mobile phase consisted of 0.1% (v/v) formic acid in water (Eluent A) and 0.1% (v/v) formic acid in acetonitrile (Eluent B). The eluent program was as follows: 20% A at 0 min, 35% A at 10 min, 55% A at 11 min, 55% A at 12 min, 0% A at 13 min, 0% A at 14 min, and 20% A at 15 min. A standard calibration was performed using MLG43 (O-BGTRIB; Megazyme) and Cello3 (O-CTR; Megazyme), and quantification was based on the 527 *m/z* ion [M + Na$^+$]. The chromatogram and spectra were processed using MassLynx software (Waters).

SDS-PAGE and Western blot

Zoseptoria tritici was cultured in YPD medium for 6 d as described above. After centrifugation at 3273 ***g*** for 15 min at 4°C, culture supernatants were filtered through 0.22 µm filters and concentrated 20-fold using Amicon Ultra centrifugal filter units with a 3 kDa molecular weight cutoff (UFC9003; Merck). Proteins were separated by SDS-PAGE on 4–20% precast polyacrylamide gels (4561094; Bio-Rad) and transferred to a nitrocellulose membrane using iBlot3 Transfer Stacks Mini NC (IB33002; Thermo Fisher Scientific, Waltham, MA, USA). The membrane was blocked in 7.5% w/v milk in blocking buffer (phosphate buffered saline with 0.1% v/v Tween 20, PBST) for 1 h at room temperature and incubated overnight at 4°C with a mouse monoclonal anti-HA antibody (H3663-200UL; Sigma-Aldrich) diluted 1 : 1000 in 5% w/v milk in PBST. Following three washes with PBST, the membrane was incubated for 1 h with the horseradish peroxidase-conjugated anti-mouse secondary antibody (A9044-2ML; Sigma-Aldrich) diluted 1 : 6000 in 5% w/v milk in PBST. Chemiluminescent signals were detected using the Pierce ECL Western Blotting Substrate kit (32209; Thermo Scientific) and acquired with the iBright FL1000 imaging system (Invitrogen). To verify equal protein loading, the samples were run on an SDS-PAGE gel and stained with 0.1% w/v Coomassie Brilliant Blue R-250. The gel image was acquired using a flatbed scanner (CanoScan LiDE 400).

Gene expression analysis

Fifteen-day-old wheat plants from the cultivar Titlis were treated, as described above, with 0.5 mM MLG43, 0.5 mM Cello3 or the mock control (0.1% v/v UEP-100; Croda and 0.01% v/v Tween 20) for 3 h. Additionally, plants were spray-inoculated with the mock solution, with the WT strain and the overexpression mutant line *ZtGH45_OE*, as described above. Three independent biological replicates, each consisting of second leaves, processed as described in 'Characterization of *in planta* β-glucan

oligosaccharide production' per treatment were used. Total RNA was extracted using the TRIzol® reagent (Invitrogen; Cat. No. 15596018), treated with DNase I (Qiagen; Cat. No. 792256) and purified using the RNeasy Plant Mini Kit (Qiagen; Cat. No. 74904) according to the manufacturer's protocol. cDNA was synthesised using the Transcriptor First Strand cDNA Synthesis Kit (Roche Applied Science, Mannheim, Germany). Quantitative reverse transcription–polymerase chain reaction (qRT-PCR) experiments were performed as previously described (Meile *et al.*, 2020) using the specific primers listed in Table S2. RNA quality check, library preparation (nonstranded polyA enrichment), and subsequent sequencing were performed by Novogene (Beijing, China) using the Illumina NovaSeq 6000 platform. The raw RNAseq reads were deposited in the NCBI Sequence Read Archive (SRA) under the BioProject accession number PRJNA1276321. About 30 million paired reads of 150 base pairs (bp) per sample were obtained. More than 95% and 1% of the reads were aligned to the *T. aestivum* (GCA_018294505) and the *Z. tritici* ST99CH_3D7 (GCA_900091695) reference genomes (available in Ensembl Plants and Ensembl Fungi), respectively, using the STAR aligner with predetermined parameters (Table S3; Dobin *et al.*, 2013). Uniquely mapped reads were counted using FeatureCounts (Liao *et al.*, 2014) in the case of wheat genes and Kallisto (Bray *et al.*, 2016) in the case of *Z. tritici* genes with default parameters. Differentially expressed genes (DEGs; Log_2-fold change = ± 0.58 with adjusted P value <0.05) were identified in each comparison using DESeq2 (Love *et al.*, 2014). Gene ontology (GO) enrichment analysis was performed using The Gene Ontology Resource tool (https://geneontology.org/) against the biological process annotation dataset. Significantly enriched GO terms were identified with PANTHER overrepresentation test using a Fisher's exact test with false discovery rate correction ($P < 0.05$).

Reactive oxygen species quantification

Discs (12.6 mm^2) from second leaves of 2-wk-old wheat plants of Titlis, Fielder, and Paragon cultivars were incubated for 16 h in the dark and at 15°C in 100 µl of a solution containing 150 µM Luminol L-012 (12-0-04891; FUJIFILM Wako Pure Chemical Corp., Osaka, Japan) and 30 µg ml^{-1} peroxidase from horseradish (P6782; Sigma-Aldrich). Fifty microlitres of 300 µM MLG43, 300 µM Cello3, 300 µM hexaacetylchitohexaose, 3 µM flg22, or H_2O were added to the discs, and the luminescence was measured using a Varioskan Lux luminescence reader (Thermo Scientific). ROS production was estimated as relative luminescence units (RLU) over time. At least 8 leaf discs per treatment were used in each experiment. The experiment was performed three times independently.

Stomatal aperture measurement

Wheat epidermal peels isolated from 2-wk-old plants were incubated in a buffer containing 50 mM KCl, 10 mM MES, 10 mM $CaCl_2$, and pH 6.25 under light for 14 h to open stomata. Subsequently, the epidermal peels were treated with 0.5 mM MLG43, 0.5 mM Cello3, 10 µM abscisic acid (ABA), or deionised water for 6 h. ABA was used as a positive control for inducing stomatal closure (Hsu *et al.*, 2021). Images of each stoma were captured with a MikrOkular Full HD camera (Bresser, GmbH, Rhede, Germany) attached to a Labophot-2 microscope (Nikon Corp., Tokyo, Japan) using CamLab Lite software. Stomatal width and length were measured using ImageJ (Schneider *et al.*, 2012). The experiment was repeated three times independently.

Synteny plot and population analyses

To assess the genomic environment of *ZtGH45*, we compared synteny in the 50-kb region surrounding *ZtGH45* in three reference genomes of *Z. tritici* strains: 3D7, 3D1, and 1E4 assemblies (Plissonneau *et al.*, 2018). For this, we used a previous annotation of orthologous genes using PoFF, a tool that integrates conserved synteny information to infer orthologous relationships (Lechner *et al.*, 2011). We integrated the transposable element annotation previously described (Lorrain *et al.*, 2021) into a synteny plot designed with the R package ggplot2 v.3.5.0 (Wickham, 2016).

To investigate the genetic variability found within the *ZtGH45* coding sequence, we examined the polymorphism found in a Swiss *Z. tritici* population of more than 800 strains (Lorrain *et al.*, 2024). We used the variant calling results from Lorrain *et al.* (2024) and extracted the genomic region corresponding to the *ZtGH45* gene (*ZtIPO323_110030*; Lapalu *et al.*, 2023). We identified the single nucleotide polymorphism (SNP) variants with a predicted nonsynonymous effect, using SnpEff (Cingolani *et al.*, 2012) with a custom database based on the latest gene annotation of the reference genome IPO323 (Lapalu *et al.*, 2023).

Statistical analysis

Data sets were statistically analysed with Prism 9 software (GraphPad Software, San Diego, CA, USA). First, outliers were detected using the ROUT method (Q = 1%), and the Gaussian distribution of the data was tested using the Shapiro–Wilk and Kolmogorov–Smirnov tests. Comparisons between two groups were performed by two-tailed t-tests. Comparisons between multiple groups that were normally distributed were performed by parametric ordinary one-way ANOVA, followed by the Dunnett test or ordinary two-way ANOVA followed by the Šídák test. Comparisons between multiple groups that were nonnormally distributed were performed by the nonparametric Kruskal–Wallis test together with Dunn's test. Raw data are available in Dataset S1.

Results

Mixed-linked glucan oligosaccharides are released during *Z. tritici* infection of wheat

To mechanistically explore how *Z. tritici* interacts with wheat cell walls, we monitored the accumulation of β-glucan oligosaccharides (MLG- and cellulose-derived oligosaccharides) during wheat

infection. We collected *Z. tritici* (strain 3D7)-infected and non-infected (Mock) wheat leaves at different time points (6, 8, and 10 dpi) and evaluated the presence of β-glucan oligosaccharides with low degrees of polymerisation (DP; Fig. S2). We quantified in these samples the well-described PTI activators β-glucan trisaccharides (MLG43 and Cello3) using hydrophilic interaction liquid chromatography in combination with electrospray ionisation-mass spectrometry (HILIC-ESI-MS; Figs 1a,b, S2). *Zymoseptoria tritici* infections led to the release of the MLG-derived oligosaccharide MLG43, which displayed maximum levels with the first appearance of the lesions (10 dpi; Fig. 1b,c). Additional putative β-glucan oligosaccharides of higher DP were detected (Fig. S2). Remarkably, the levels of the main expected potential products derived from cellulose degradation, cello-oligosaccharides, did not increase during infection (Fig. 1b). To determine the origin of the detected MLG43 during *Z. tritici* infection of wheat, we evaluated the presence of β-1,3/1,4-glucan in the cell walls of both wheat and *Z. tritici*. In leaves of 17-d-old wheat plants, β-1,3/1,4-glucan accounted for 0.8% (7.8 ± 0.6 mg g^{-1}) of the cell wall (Alcohol Insoluble Residue; AIR), whereas β-1,3/1,4-glucan was not detected in *Z. tritici* AIR. These results point to wheat as the sole source of the observed release of β-1,3/1,4-glucan oligosaccharides. Overall, the results indicate that β-1,3/1,4-glucan-derived oligosaccharides are released from wheat cell walls during *Z. tritici* infection.

We next aimed to identify the CAZyme(s) secreted by *Z. tritici* which led to the production of MLG43. We hypothesised that enzymes leading to MLG43 accumulation should have a predicted glucanase activity (EC 3.2.1.4) and be highly expressed at the beginning of the necrotrophic phase. Of the 27 *Z. tritici* genes encoding GHs with a predicted glucanase activity (from the families GH5, GH7, GH10, GH12, GH45, and GH51), one (*ZtGH45*/*Zt3D7_G10118*) displayed very low expression levels at 7 dpi and when grown under axenic conditions, but was highly induced at the necrotrophic phase, and exhibited expression levels that remained high during this phase (12–28 dpi; Figs S3, S4a; Palma-Guerrero *et al.*, 2017; Francisco *et al.*, 2019). We checked whether *ZtGH45* was also present in other *Z. tritici* strains. Indeed, in the strains 3D1 and 1E4, *ZtGH45* was also present in chromosome 10 (Fig. S4d). We additionally used a previously published RNAseq dataset performed with the strains 3D1 and 1E4 (Palma-Guerrero *et al.*, 2017) to evaluate the expression of *ZtGH45* in these strains. These strains have a slower infection rate than 3D7, 3D1 being a slower coloniser than 1E4 (Palma-Guerrero *et al.*, 2017). Accordingly, we observed that in 1E4, *ZtGH45* was expressed slightly lower at 12 dpi than in 3D7, and that in 3D1, *ZtGH45* expression was increased only at 14 dpi (Fig. 1d). Thus, *ZtGH45* is expressed at the necrotrophic phase for these three strains.

*Zt*GH45 harbours six cysteine bridges, as shown in an ALPHAFOLD2 model, is highly polymorphic and was previously shown to be under significant diversifying selection (Fig. S4e,f; Brunner *et al.*, 2013). Despite the high number of polymorphic residues of *Zt*GH45, the critical residues for GH45 activity (D37 and D145), as reported in *Neurospora crassa* and *Thermothielavioides terrestris* (Gao *et al.*, 2017; Kadowaki & Polikarpov, 2019), were shown to be conserved in all the investigated strains of *Z. tritici*, suggesting a potential β-1,4-glucanase activity of *Zt*GH45 (Fig. S4c,f).

Impact of constitutive *ZtGH45* expression on *Z. tritici* virulence

We functionally characterised *Zt*GH45 by obtaining mutant lines in which *ZtGH45* was disrupted. The three tested independent knockout lines (Δ*gh45*) did not show differences in virulence compared to the control (Fig. S5a,b). We also obtained overexpression lines in which we substituted the native promoter with the constitutive *gdpA* promoter (*ZtGH45*-overexpression line *in locus*, *ZtGH45_OE*). In the WT control, *ZtGH45* is not expressed under axenic conditions and has low expression levels at the early stages of the infection, as previously reported (Meile *et al.*, 2020; Suarez-Fernandez *et al.*, 2023; Figs 1e, S4a). By contrast, in the *ZtGH45_OE* line, *ZtGH45* expression levels remained high throughout the *Z. tritici* infection cycle (Figs 1e, S4b, S5c). The three tested *ZtGH45_OE* lines showed reduced virulence in the cultivar Titlis in comparison to the WT strain, as reflected by a reduction in the percentage of leaf area covered by lesions and by impaired reproduction, as shown by diminished pycnidia density (Figs 1f,g, S5d). This effect was not cultivar-specific since we observed a similar effect in the cultivar Drifter (Fig. S5e,f). *ZtGH45* expression levels were not significantly different between the WT and *ZtGH45_OE* lines during the necrotrophic phase (Fig. 1e). These data suggest that the reduced virulence phenotype observed in the *ZtGH45_OE* lines was attributable solely to the misexpression of the gene at the early stages of infection. To rule out the possibility that the virulence phenotype resulted from altered growth of the mutant, we conducted an *in vitro* growth analysis in minimal medium supplemented with different carbon sources (sucrose, fructose, and CMC, and barley β-glucan) and in yeast malt sucrose (YMS) medium in the presence of different abiotic stresses (sorbitol, NaCl, H_2O_2, Calcofluor white, and 28°C). No differences in growth were observed between the *ZtGH45_OE* and the WT lines (Fig. S6). These results demonstrate that misexpression of *ZtGH45* hampered the ability of *Z. tritici* to colonise the host.

We next explored whether the reduced virulence of *ZtGH45_OE* was due to the recognition of the *Zt*GH45 protein itself or due to the recognition of the released oligosaccharides from the wheat cell walls by the activity of *Zt*GH45. With this aim, we obtained a mutant line that overexpressed an enzymatically inactive version of *Zt*GH45 (*Zt*GH45_OE$^{D37A/D145A}$). As a control, we also obtained an overexpression mutant line of the WT version of *Zt*GH45 (*Zt*GH45_OE^{WT}). The gene expression levels of both the mutant and the WT version of the protein were statistically not different (Fig. S5c). We additionally obtained 3xHA-tagged *Zt*GH45^{WT} and *Zt*GH45$^{D37A/D145A}$ overexpression lines, which showed that both protein versions accumulated to similar levels, indicating that the catalytic dead version is stable (Fig. S7a). *ZtGH45_OE* $^{D37A/D145A}$ was not impaired in virulence, while *ZtGH45_OE*^{WT} hindered *Z. tritici* progression (Figs 1g, S7b–d). This effect was not cultivar-specific since it was also observed in the cultivars Fielder and Paragon (Fig. S7e,f).

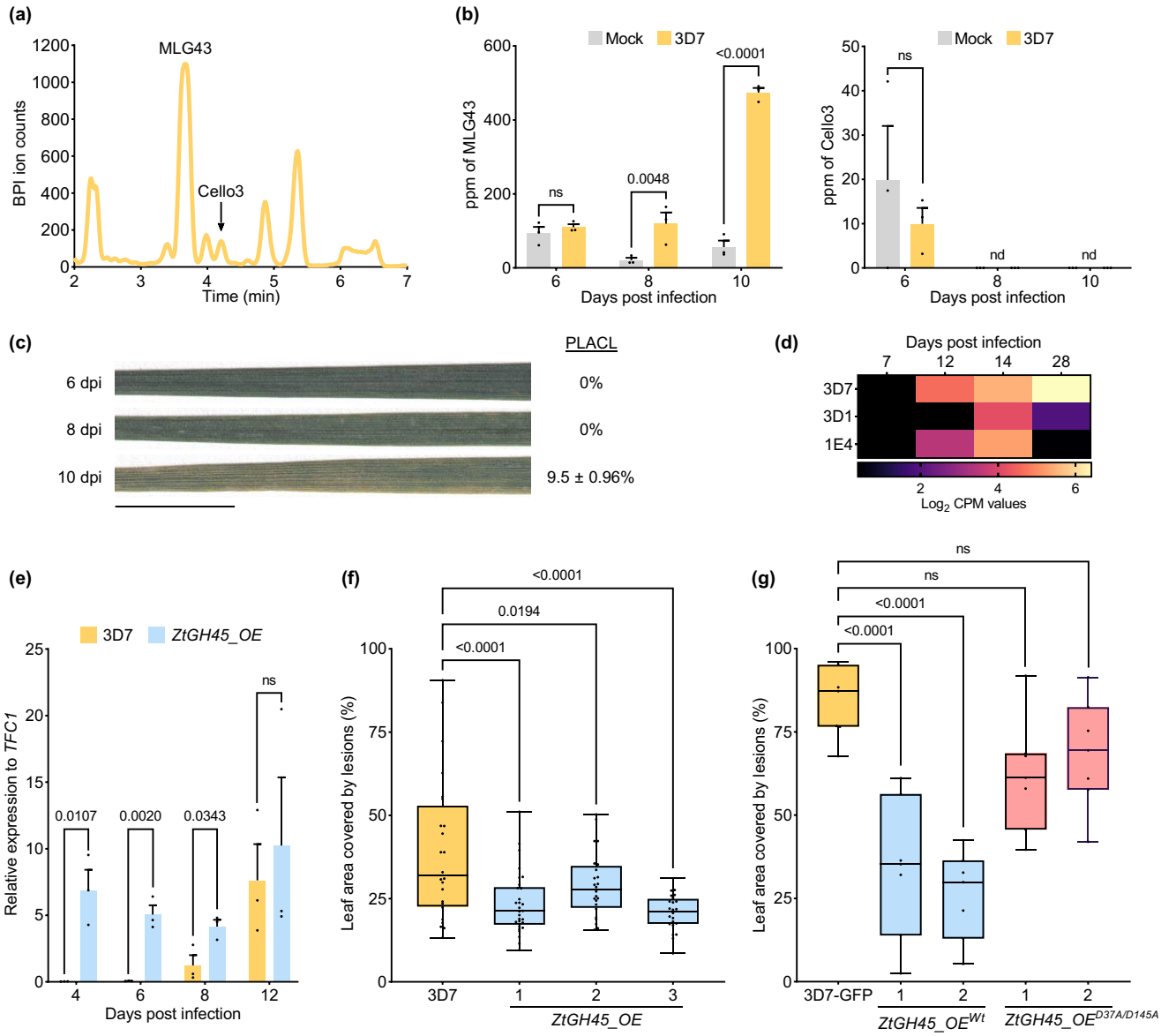

Fig. 1 Mixed-linked glucan oligosaccharides are released in wheat during *Zymoseptoria tritici* infection and early expression of *ZtGH45* hampers virulence. (a) Base peak intensity (BPI) chromatogram obtained by hydrophilic interaction liquid chromatography coupled to electrospray ionisation-mass spectrometry (HILIC-ESI-MS) of wheat leaf extracts at 10 d post infection (dpi) with 10^7 spores ml^{-1} of wild-type (WT) strain ST99CH_3D7 (3D7) of *Z. tritici*. β-D-cellobiosyl-1,3-β-D-glucose (MLG43) mean peak and cellotriose (Cello3) peak are labeled. (b) Quantification by HILIC-ESI-MS of the mixed-linked glucan-derived oligosaccharides MLG43 (left) and Cello3 (right) released at 6, 8, and 10 dpi with 10^7 spores ml^{-1} of 3D7. *P*-values according to two-way ANOVA followed by Šídák test between plants infected with the 3D7 strain and mock-treated plants are displayed in the plots. Values below the detection limit are expressed as not detected (nd). The results are from three biological replicates and errors represent SE. (c) Images of leaf sections of wheat plants infected with 3D7 (10^7 spores ml^{-1}) at 6, 8, and 10 dpi. The average of the percentage of leaf area covered by lesions (PLACL ± SE of the mean) of the first 17 cm from the tip is indicated next to each picture. Bar, 1 cm. This experiment was repeated twice. (d) Expression levels of *ZtGH45* in the *Z. tritici* strains 3D1, 3D7, and 1E4 at 7, 12, 14, and 28 dpi. Data were obtained from a previously published RNA-seq study (NCBI accessions: SRA SRP077418). Note that the virulence of 3D7 is higher than that of 1E4 and 3D1. (e) Expression pattern of *ZtGH45* in the WT strain 3D7 (yellow bars) and in the lines constitutively overexpressing *in locus ZtGH45* (*ZtGH45_OE*, blue bars) during wheat (cultivar Titlis) infection (10^7 spores ml^{-1}) at 4, 6, 8, and 12 dpi. Values shown are relative to the *Z. tritici* housekeeping gene *TFC1*. *P* values according to a two-tailed *t*-test between plants infected with the *ZtGH45_OE* line and the 3D7 strain are displayed in the plots. Data are from three biological replicates. Errors represent SE of the mean. (f) Percentage of leaf area covered by lesions produced by the infection (10^7 spores ml^{-1}) with 3D7 (control, yellow bar) and *ZtGH45_OE* (blue bars; *in locus* mutant) lines at 13 dpi on wheat plants of cultivar Titlis. The experiment was performed three times with line #3 and we obtained similar results. (g) PLACL produced by the infection (5×10^6 spores ml^{-1}) in wheat plants (cultivar Titlis) by 3D7-GFP (control, yellow bar) and lines ectopically overexpressing the *ZtGH45* WT version (*ZtGH45_OE*^{WT}; blue bars) or *Zt*GH45 with the catalytic site mutated (*ZtGH45_OE*$^{D37A/D145A}$; red bars; ectopic mutants) at 13 dpi. In both (f, g), the *P* values according to a one-way ANOVA followed by Dunnett test between plants infected with the mutant lines and the control strain are displayed in the plots. In the boxplots, the middle line and the box represent the median and the interquartile range, respectively. Whiskers extend to the minimum and maximum values, and each black dot represents an individual datapoint. ns indicates non significant differences.

The results demonstrate that the phenotype of *ZtGH45_OE*^{WT} is exclusively attributable to the catalytic activity of *Zt*GH45, and that the wheat immune system does not recognise the protein itself.

Constitutive expression of *ZtGH45* leads to enhanced release of MLG-derived oligosaccharides

We further explored the capacity of *Zt*GH45 to release β-glucans. We cultivated *Z. tritici* WT and three independent *ZtGH45_OE* lines in the presence of 0.5% (w/v) β-1,3/1,4-glucan or β-1,4-glucan (CMC). β-glucan oligosaccharide quantification of the culture filtrates after 96 h of growth revealed that the *ZtGH45_OE* line significantly released more β-glucan oligosaccharides than the WT strain when employing β-1,3/β-1,4-glucan as a substrate (39%, 51%, and 66% for each independent *ZtGH45_OE* line and 15% for the WT; % w/w of the initial material), and these levels were similar to those generated by incubating MLG with a commercial cellulase (Fig. S8a). When using CMC as a substrate, we detected the release of β-1,4-glucan oligosaccharides (0.2% of the initial material; w/w) only in the *ZtGH45_OE* lines and not in the WT strain (Fig. S8b). To assess the contribution of the catalytic activity to the release of oligosaccharides, we grew the knockout (Δ*gh45*) and the ectopic lines overexpressing either the WT or the catalytic dead version (*ZtGH45_OE*^{WT} and *ZtGH45_OE*$^{D37A/D145A}$) in the presence of 0.5% (w/v) β-1,3/1,4-glucan. As expected, we observed that only the overexpression line of the WT *ZtGH45* led to an enhanced release of β-glucans compared to the control line (3D7-GFP; Fig. 2a), indicating that ZtGH45 catalytic activity is key for the hydrolysis of β-1,3/1,4-glucan. To bring the experimental conditions closer to the *in vivo* wheat environment, the control line (3D7-GFP) and the mutant lines were grown in the presence of wheat cell wall fraction (AIR) obtained from 17 d-old seedlings. β-1,3/1,4-glucan- and β-1,4-glucan-derived oligosaccharides were released by all the lines tested, but the *ZtGH45_OE*^{WT} line released 2.4-fold higher levels of β-glucan oligosaccharides than 3D7-GFP (Fig. 2b). The knockout and the catalytic dead overexpression lines released similar levels of the oligosaccharides as the control line (Fig. 2b). Oligosaccharides released by *ZtGH45_OE* from β-1,3/1,4-glucans were further characterised using high-performance anion-exchange chromatography with pulsed amperometric detection (HPAEC-PAD). *Zt*GH45_OE^{WT} exhibited an enhanced production of MLG43 compared to the control, the knockout mutant line, and the line overexpressing the catalytic dead version of ZtGH45 (*Zt*GH45_OE$^{D37A/D145A}$; Figs 2c, S8c). These findings corroborate that β-1,4-glucanase activity of *Zt*GH45 contributes to the hydrolysis of β-1,3/1,4-glucan from the wheat cell wall, leading to the release of β-glucan oligosaccharides.

Mixed-linked glucan oligosaccharides trigger wheat immunity

We hypothesised that the impaired virulence of the *ZtGH45_OE* lines was due to an early *Zt*GH45-dependent release of β-glucan oligosaccharides. To test this hypothesis, we investigated whether *Zt*GH45-derived oligosaccharides function as plant immunity-activating molecular patterns. MLG43 treatment of wheat leaves 24 h before inoculation with the WT strain resulted in a reduction in symptoms and pycnidia formation compared to mock-treated plants in the cultivar Titlis after 14 d of infection (Figs 2d,e, S8d). Cello3 also led to a reduction in symptom development and a slight reduction in pycnidia formation (Figs 2d,e, S8d). These results suggest that these β-glucan oligosaccharides prime wheat plants against pathogen attack.

To determine whether these cell wall-derived oligosaccharides induced transcriptional reprogramming in wheat, including the activation of defence-related genes, we performed a comparative wheat transcriptomic analysis in plants 3 h after treatment with either MLG43, Cello3, or the mock solution. In the principal component analyses, MLG43-induced transcriptional changes compared to mock were primarily captured by PC1, explaining 88% of the total variance, while Cello3-associated changes were delineated by PC2, which accounted for 4% of the total variance (Fig. S9a). Surprisingly, this observation indicates that MLG43 triggers a more pronounced transcriptional reprogramming in wheat plants compared to Cello3. Accordingly, when comparing the transcriptomic profiles of treated and control samples, we identified a total of 26 (20 upregulated) and 3997 (3173 upregulated) DEG (foldchange (Log_2) ± 0.58, *P*-adjusted value ≤ 0.05) upon treatment with Cello3 and MLG43, respectively. Of these, 17 genes were differentially expressed upon both treatments, indicating that the two oligosaccharides elicit distinct transcriptomic responses or, alternatively, that the response to Cello3 may occur at a different time point (Tables S4, S5). Consistent with its role as a DAMP, the 3173 genes upregulated upon MLG43 treatment were enriched in GO terms related to disease resistance responses ('innate immune response' (GO:0045087), 'defence response to other organism' (GO:0098542), and 'transmembrane receptor protein serine/threonine kinase signalling pathway' (GO:0007178; Table S6)) and included 178 genes encoding for defence-related proteins, consisting of homologues of 22 chitinases and 149 receptor kinases, including CERK1, CEBiP (chitin elicitor-binding protein), LYK5 (LysM motif receptor kinase 5), one LRR-MAL receptor kinase, 21 LRR receptor kinases, six wall-associated receptor kinases (WAK), and 23 LecRKs (Table S7). Remarkably, cell wall-related GOs (GO:0071554 and GO:0044036) were also significantly enriched in the genes induced by MLG43 (Table S6). Overall, the results suggest that MLG43 treatment leads to a transcriptional reprogramming involving the induction of an immune response and cell wall remodelling.

In parallel, we also investigated the transcriptional response of wheat plants to infection with the line constitutively expressing *ZtGH45* (*ZtGH45_OE*). Samples from WT (3D7)-infected, *ZtGH45_OE*-infected, and non-infected control plants were collected at an early stage of infection (6 dpi), when no macroscopic symptoms were yet visible (Bernasconi *et al.*, 2023; Alassimone *et al.*, 2024), and the WT strain did not express *ZtGH45*. The principal component analysis highlighted that infection with

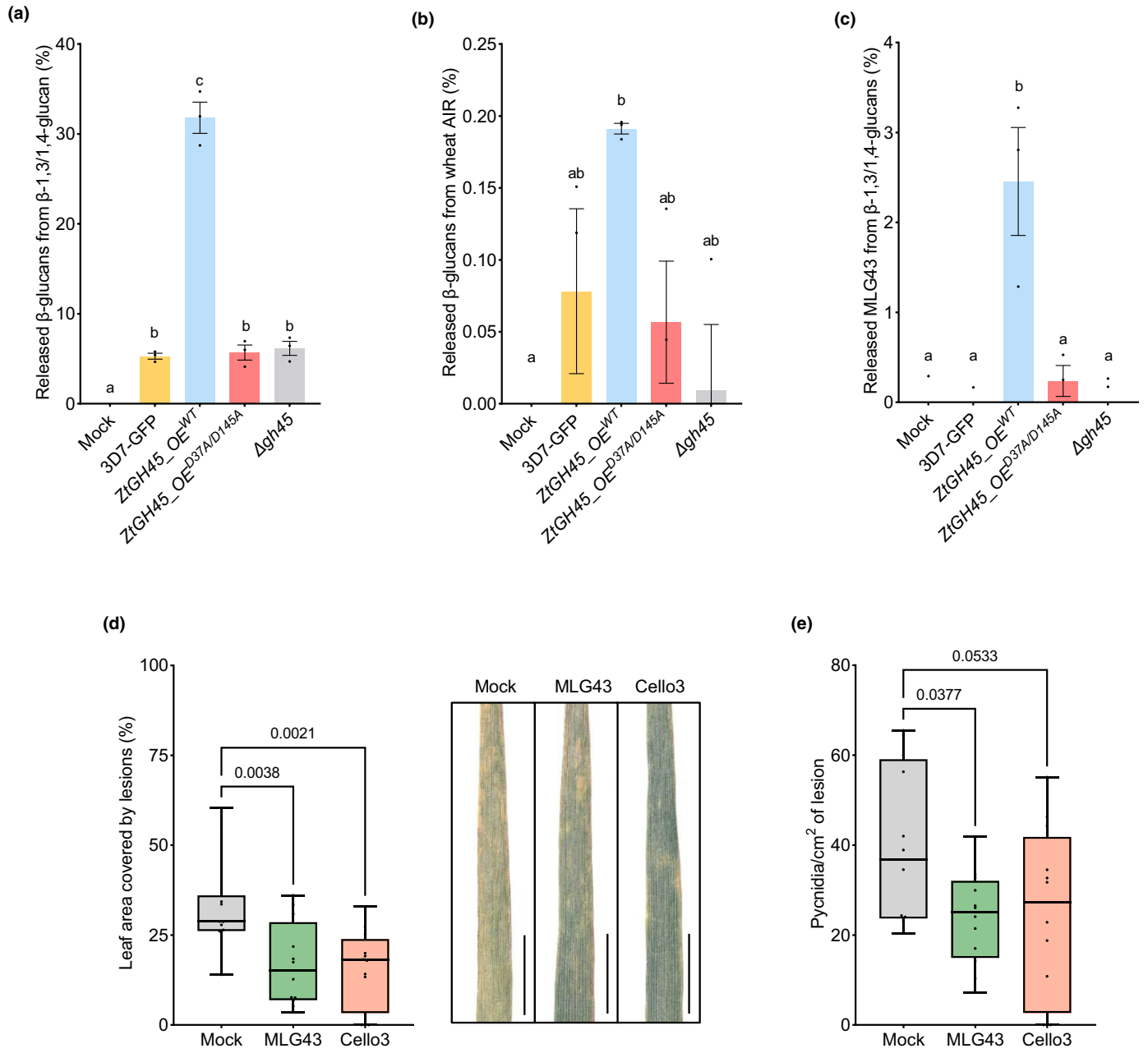

Fig. 2 *ZtGH45* overexpression leads to an enhanced degradation of wheat cell wall β-glucan polysaccharides and to the release of oligosaccharides that trigger resistance against *Zymoseptoria tritici*. (a, b) β-glucan oligosaccharides released by *Zymoseptoria tritici* 3D7-GFP (background control), the knockout of *ZtGH45* (*Δgh45*), and the mutant lines overexpressing the wild-type (WT) version of *ZtGH45* (*ZtGH45_OE*^{WT}), and the catalytic dead version of *ZtGH45* (*ZtGH45_OE*$^{D37A/D145A}$) grown in Vogel's minimal medium supplemented with 0.5% (w/v) fructose and with either 0.5% (w/v) barley mixed-linked glucan polysaccharide (β-1,3/1,4-glucan) (a) or 0.5% (w/v) wheat alcohol insoluble residue (AIR) (b). Oligosaccharides were quantified after 96 h (a) or 120 h of growth (b). (c) β-D-cellobiosyl-1,3-β-D-glucose (MLG43) released by 3D7, *ZtGH45_OE*, *ZtGH45_OE*$^{D37A/D145A}$, and *Δgh45* lines after 96 h of growth in β-glucan-supplemented media quantified by high-performance anion-exchange chromatography with pulsed amperometric detection (HPAEC-PAD). Bars shown in (a–c) panels represent the mean of three biological replicates, and the error bars represent the SE of the mean. Different letters indicate significant differences (*P* value <0.05) according to one-way ANOVA followed by Šídák multiple comparison test. (d, e) *Zymoseptoria tritici* strain 3D7 virulence measured as a percentage of leaf area covered by lesions (d) and pycnidia density (pycnidia cm^{-2} of lesion) (e) at 14 d post infection (dpi) with 5 × 10^6 spores ml^{-1} in Titlis wheat plants pretreated with 0.5 mM β-D-cellobiosyl-1,3-β-D-glucose (MLG43; green bar) or 0.5 mM cellotriose (Cello3; red bar) 24 h before infection. *P* values according to one-way ANOVA followed by Dunnett test between the oligosaccharide treatments and the mock control are displayed in the plots. In the boxplots, the middle line and the box represent the median and the interquartile range, respectively. Whiskers extend to the minimum and maximum values, and each black dot represents an individual datapoint. One representative picture of each treatment is shown in (d). Bars, 1 cm. An additional replicate of the results presented in (e) is shown in Supporting Information Fig. S8(d).

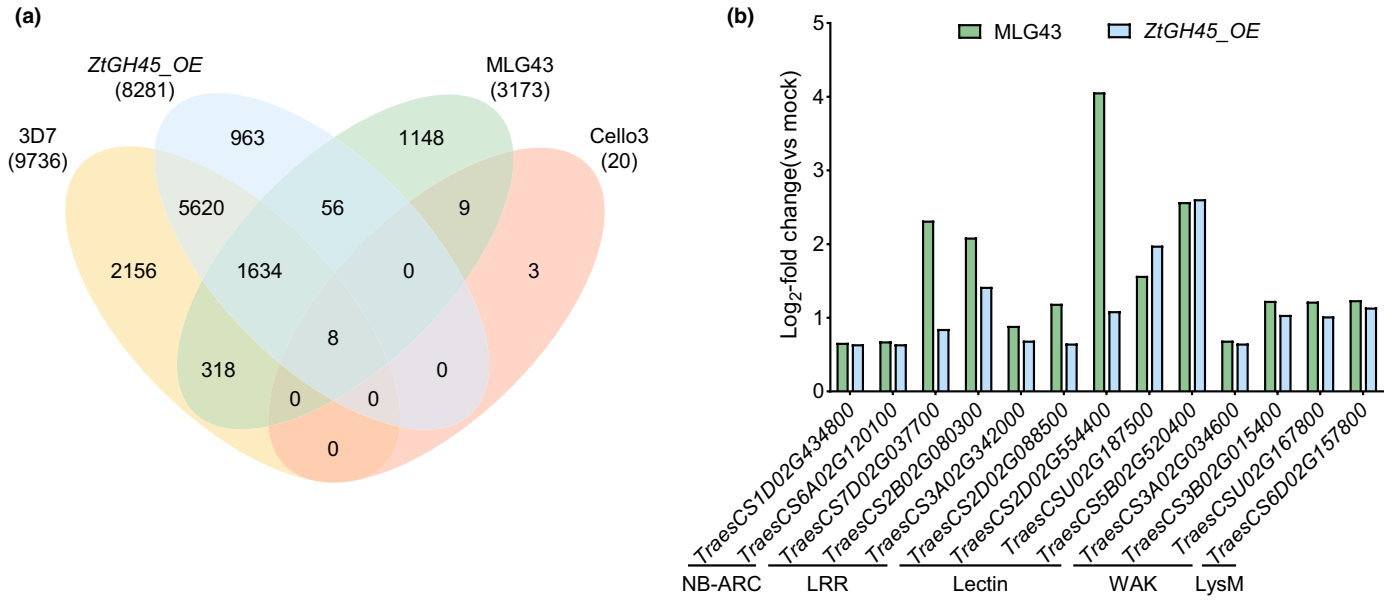

Fig. 3 Mixed-linked glucan oligosaccharides trigger a defense response in wheat. (a) Venn diagram representing shared and distinct significant upregulated genes in wheat plants upon infection (10^7 spores ml^{-1}) with *Zymoseptoria tritici* 3D7 or *ZtGH45_OE* or upon treatment with 0.5 mM β-D-cellobiosyl-(1,3)-β-D-glucose (MLG43) or 0.5 mM cellotriose (Cello3). Wheat transcriptomes were analysed 3 h after treatment with the oligosaccharides or at 6 d after infection. (b) Log_2 fold change levels of potential resistance genes upregulated by 0.5 mM MLG43 (green bars; 3 h after treatment) and by infection with *ZtGH45_OE* (blue bars; 6 dpi). Upregulated genes encoding putative resistance genes (NB-ARC-containing proteins) and receptors from different families (Lectin, LysM, Leucine Rich Repeat (LRR), and wall-associated receptor kinases (WAK)) are shown.

the WT and the *ZtGH45_OE* lines led to changes in the transcriptome compared to the mock, explaining 90% of the total variance (Fig. S9b). In total, 20 451 and 17 375 wheat genes were differentially expressed upon infection with the WT and the overexpression line, respectively, compared to the control plants, of which 14 940 genes were shared and 2435 were specific to *ZtGH45_OE* infection (Tables S4, S5). Of the total upregulated genes upon infection, we identified 1019 genes (12.3%) that were induced only upon *ZtGH45_OE* infection (Fig. 3a; Table S8). These genes specifically induced upon *ZtGH45_OE* infection were enriched in 'regulation of β-glucan biosynthetic process' (GO:0032951), 'response to other organisms' (GO:0051707), and 'phosphorylation' (GO:0016310) GO terms (Table S9). Among these genes, two encoded for 1,3-β-glucan synthases, 26 for receptor-like kinases (Table S8). From the fungal side, only seven genes were differentially regulated in the *ZtGH45_OE* line compared to the WT strain (Tables S10, S11).

We further evaluated if the transcriptomic profiles of the *Z. tritici* and MLG43 treatments overlapped. We found that > 60% (2016) of the genes upregulated by MLG43 were also induced upon *Z. tritici* infection, and that *c.* 50% (1698) of the upregulated genes by MLG43 were induced by *ZtGH45_OE* (Figs 3a, S9c). Of these, 56 genes were specifically regulated by *ZtGH45_OE* and not by the 3D7 WT strain, including 13 genes involved in stress perception and signalling (Fig 3b; Table S12). Overall, we identified a set of wheat defence-related genes induced after treatment with MLG43 and infection with *ZtGH45_OE*.

MLG43 triggers a ROS burst and stomatal closure

In *Arabidopsis thaliana*, respiratory burst oxidase (RBOH) produces ROS upon MAMP recognition (Torres *et al.*, 2002). Since five wheat respiratory burst oxidase (*RBOH*) homologues were upregulated upon MLG43 treatment (Fig. 4a), we quantified ROS accumulation upon treatment with this elicitor in cultivar Titlis. We used either chitohexaose (O-CHI6) or flg22 as positive controls since they both trigger ROS accumulation in wheat (Fig. S9d, e). We observed that wheat leaves underwent a ROS burst upon treatment with MLG43 (Fig. 4b, c). Remarkably, a ROS burst was also observed in cultivars Fielder and Paragon, indicating that MLG43 triggers this immune response regardless of the wheat cultivar used (Figs 4d,e, S9f,g). By contrast, wheat treated with Cello3 did not undergo ROS accumulation (Figs 4b,c, S9f,g). Additionally, the transcriptomic analysis also revealed an upregulation of 15 genes involved in stomatal closure regulation, encoding for homologues of two SLAH3 (Liu *et al.*, 2019), eight plant glutamate receptors (Kong *et al.*, 2016), four calcium-dependent protein kinases (Geiger *et al.*, 2010; Brandt *et al.*, 2012; Scherzer *et al.*, 2012), and one CBL-interacting protein kinase (Fig. 4a; Förster *et al.*, 2019), suggesting that MLG43 might regulate stomatal closure. Since stomata have been shown to play a pivotal role in plant resistance and are the major entry gate for *Z. tritici* to the apoplast (Battache *et al.*, 2022, 2024; Bernasconi *et al.*, 2023), we investigated whether *Zt*GH45-released cell wall oligomers regulate stomatal movements by treating wheat leaves with MLG43 and Cello3 and assessing stomatal opening.

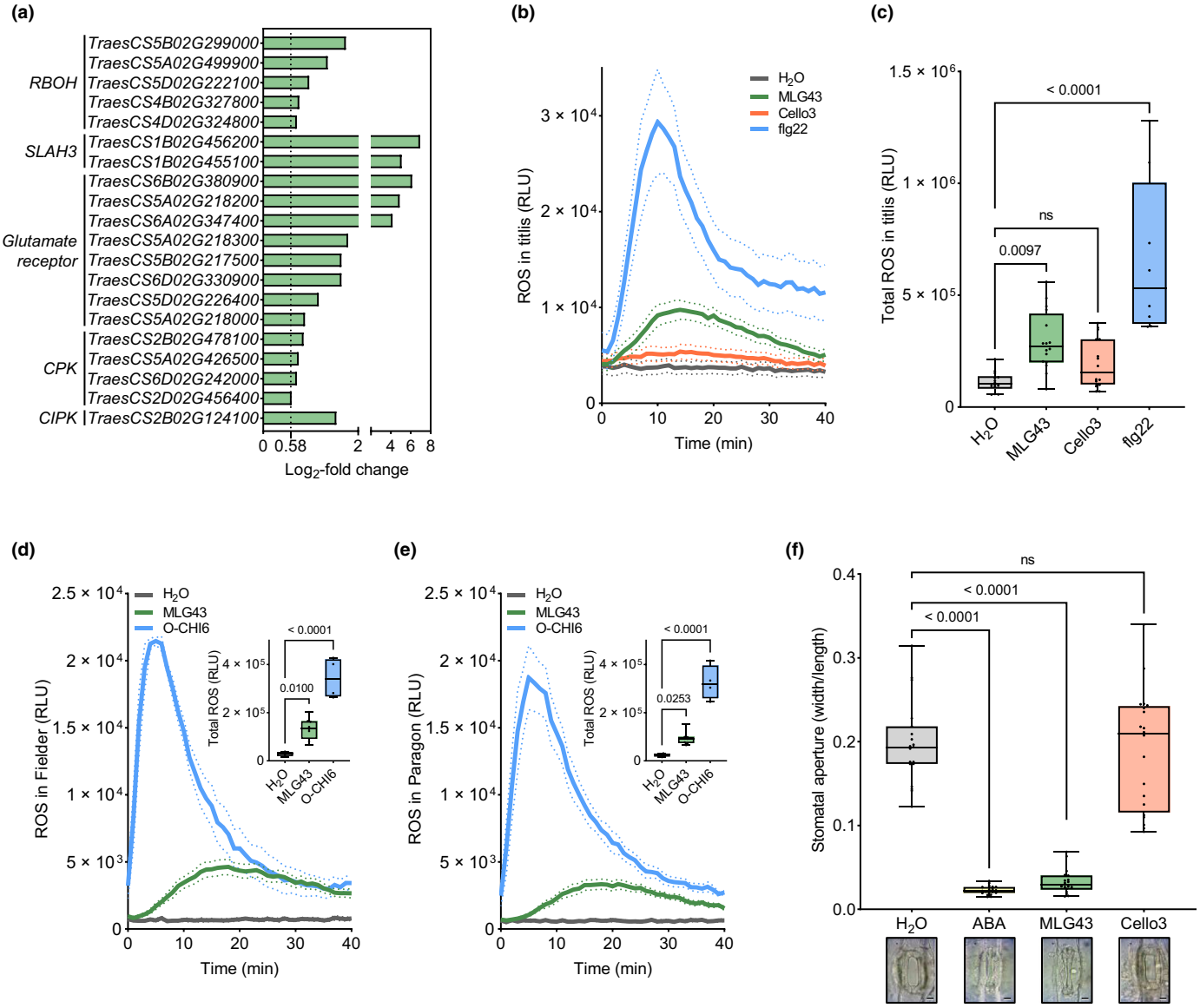

Fig. 4 Mixed-linked glucan oligosaccharides trigger reactive oxygen species (ROS) burst and stomatal closure in wheat plants. (a) Expression levels of stomatal immunity-related genes in wheat plants treated with MLG43. Log_2-fold change compared to mock is represented. (b) ROS production in wheat leaf discs of cultivar Titlis upon treatment with 100 μM MLG43 or cellotriose (Cello3) measured as relative luminescence units (RLU) over time. One microMolar flagellin-derived 22-amino-acid epitope (flg22) was used as a positive control. Dashed lines represent the SE of the mean. (c) Total ROS production estimated as cumulative RLUs over 40 min in cultivar Titlis. These experiments were repeated twice and gave similar results. (d, e) ROS production, estimated as RLUs, in wheat leaf discs of cultivar Fielder (d) and Paragon (e) upon treatment with 100 μM MLG43 or 100 μM hexaacetyl-chitohexaose (O-CHI6), used as a positive control. Total ROS production is shown in the right upper corner. In (b–e), water was used as a negative control and in (c–e), significant differences (*P* values according to one-way ANOVA followed by Dunnett test) with the negative control (H_2O) are displayed in the plots. (f) Stomatal closure in response to MLG43. Boxplots represent the width : length ratio of the stomatal pore, as a proxy for stomatal aperture, in wheat epidermal peels treated with 0.5 mM of MLG43 or 0.5 mM Cello3 for 6 h. Water and 10 μM abscisic acid (ABA) were used as negative and positive controls, respectively. *P* values according to Kruskal–Wallis test followed by Dunn test between MLG43, Cello3, or ABA treatment and H_2O are displayed in the plots. This experiment was repeated twice and gave similar results. Representative images of stomata exposed to 10 μM ABA, 0.5 mM MLG43, or 0.5 mM Cello3 for 6 h are shown. Bars, 10 μm. In the boxplots, the middle line and the box represent the median and the interquartile range, respectively. Whiskers extend to the minimum and maximum values, and each black dot represents an individual datapoint. ns indicates non significant differences.

Remarkably, we observed that wheat plants closed their stomata 6 h after MLG43 treatment, mimicking the response induced by ABA, which was used as a positive control (ABA; Fig. 4f; Hsu *et al.*, 2021). By contrast, stomata remained open upon Cello3 and water treatment (Fig. 4f). These results indicate that the recognition of MLG43 triggers an immune response and leads to ROS accumulation and subsequent stomatal closure in wheat plants.

Discussion

Plant cell walls play a central role in mediating plant-pathogen interactions since they act as defensive barriers against pathogen invasion and serve as a source of nutrients for pathogens (Molina *et al.*, 2024a). Pathogens secrete an arsenal of CAZymes (including CWDEs) during their infection cycle (Brunner *et al.*, 2013; Bradley *et al.*, 2022) to modify and break down plant cell wall carbohydrate polymers, presumably to surmount the cell wall as a physical barrier and to acquire nutrients (Bradley *et al.*, 2022). As a result of CAZyme activity, cell wall-derived oligosaccharides are released and frequently detected by the host as DAMPs, triggering immune responses and hindering pathogen progression (Bacete *et al.*, 2018; Molina *et al.*, 2024a). In this work, we functionally characterised a GH from family 45 of the fungal plant pathogen *Z. tritici*, *Zt*GH45. Constitutive expression of *ZtGH45* hinders *Z. tritici* infection and leads to an enhanced release of plant cell wall-derived MLG oligosaccharides, which the wheat host recognises as immunity-activating molecular patterns. These results suggest that *Z. tritici* tightly regulates *ZtGH45*, which is expressed only during the necrotrophic phase, to delay the release of MLG oligosaccharides and prevent early recognition by the host. Our experiments demonstrate that tight regulation of pathogen CWDEs controls the release of elicitors that trigger plant resistance.

Zymoseptoria tritici- infection leads to changes in the cell wall composition, featuring an increase of oligosaccharides derived from β-1,3/1,4-glucans (MLGs). The released MLG-derived trisaccharide is immunogenic and confers protection against *Z. tritici* in wheat plants, similar to what has been described for other plant species, including rice, tomato, pepper, and *A. thaliana* (Rebaque *et al.*, 2021; Dai *et al.*, 2023). Perception of MLG43 in *A. thaliana* and rice is mediated by LysM receptor kinases, and OsLecRK1 and AtLRR-MAL RKs (IGP1/CORK1, IGP3 and IGP4) (Rebaque *et al.*, 2021; Yang *et al.*, 2021; Dai *et al.*, 2023; Martín-Dacal *et al.*, 2023). The mechanisms mediating MLG43 perception in wheat remain unknown. We speculate that a PRR directly interacts with MLG43, similar to what has been reported for other oligosaccharides acting as MAMPs/DAMPs (Martín-Dacal *et al.*, 2023), but further evidence is required to demonstrate this hypothesis. MLG43 detection leads to the activation of several defence-related genes, including three LysM-containing receptors, one LRR-MAL RK, 23 LecRKs, and six genes encoding WAKs. The upregulation of these putative receptor-encoding genes in wheat in response to MLG43 treatment suggests their potential contribution to the perception of this elicitor. However, we cannot discard that they are part of a general immune response triggered by this DAMP. Notably, 50% of MLG43-induced genes were also upregulated during infection with the *ZtGH45* overexpression line, highlighting its contribution to wheat resistance. In addition to inducing defence-related genes, MLG43 triggers the accumulation of ROS and stomatal closure in wheat, which likely limits penetration by *Z. tritici* and potentially accounts for the observed protection capacity of MLG oligosaccharides.

Remarkably, we did not detect an increase in cellulose-derived oligosaccharides upon *Z. tritici* infection. This was unexpected since the wheat cell wall is rich in cellulose. This might be due to the higher accessibility of β-1,3/1,4-glucans in the plant cell wall compared to β-1,4-glucan, which forms cellulose microfibrils (Zoghlami & Paës, 2019). Additionally, we cannot discard the possibility that cello-oligosaccharides with a low degree of polymerisation might be released but subsequently targeted by degrading enzymes, including cellodextrin oxidases, from the plant, as reported in Arabidopsis (Costantini *et al.*, 2023), and are therefore not detected. Cello3 treatment hindered symptom development by *Z. tritici* but did not lead to a significant reduction in pycnidia formation. We did not observe major transcriptomic changes in response to cellulose-derived oligosaccharides. This may reflect a distinct transcriptional profile with different temporal dynamics, such that key responses might occur outside the time point we analysed. Overall, we suggest that the mechanisms leading to MLG43 and Cello3-triggered immunity are not fully shared.

We hypothesise that during colonisation, pathogens, including *Z. tritici*, seek to minimise the generation of cell wall-derived DAMPs to enhance the infection process. Accordingly, MLG-oligomers accumulation is not observed at the early stages of the infection but increases at the later stages with the first appearance of symptoms. We propose that MLG43-triggered immune responses at this late stage – when the pathogen is already proliferating in the apoplast – are insufficient to halt disease progression. By contrast, if MLG43 were released earlier, it could effectively impede infection by triggering stomatal closure, defense gene induction, and ROS accumulation. Thus, we suggest that the expression of enzymes hydrolysing MLGs and releasing MLG-derived DAMPs (as *Zt*GH45) is repressed in *Z. tritici* during the early colonising stages of the infection as a mechanism of host evasion. Accordingly, the early expression of *ZtGH45* in the overexpression lines triggers an early induction of 26 potential PRRs, as shown in the transcriptomic analysis. In *M. oryzae*, MoCel12 hydrolyses MLG and releases MLG oligosaccharides. As we observed for *ZtGH45*, the expression levels of *MoCel12* are regulated to potentially mitigate the detection of the pathogen (Yang *et al.*, 2021). Remarkably, distinct GHs can trigger the release of the same DAMP species (Yang *et al.*, 2021; this work), underscoring the central role that β-1,3/1,4-glucans represent in the outcome of plant–pathogen interactions. Notably, *Z. tritici* has a homologue of *Mo*Cel12 (*Zt*GH12), which is also expressed at the necrotrophic phase. We suggest that *Zt*GH45 and *Zt*GH12 might contribute to the breakdown of MLGs and influence pathogen progression. The function of these two enzymes at the late stages of the infection and how they contribute to the pathogen's life cycle remains to be unveiled (Fig. 5).

Despite the low expression at the early stages of infections, *ZtGH45* is highly induced during the necrotrophic phase. Several effector genes display a similar expression pattern (Rudd *et al.*, 2015; Palma-Guerrero *et al.*, 2017), but the signal leading to the activation of these genes remains unknown. The expression pattern of *ZtGH45* suggests a role for the enzyme at the

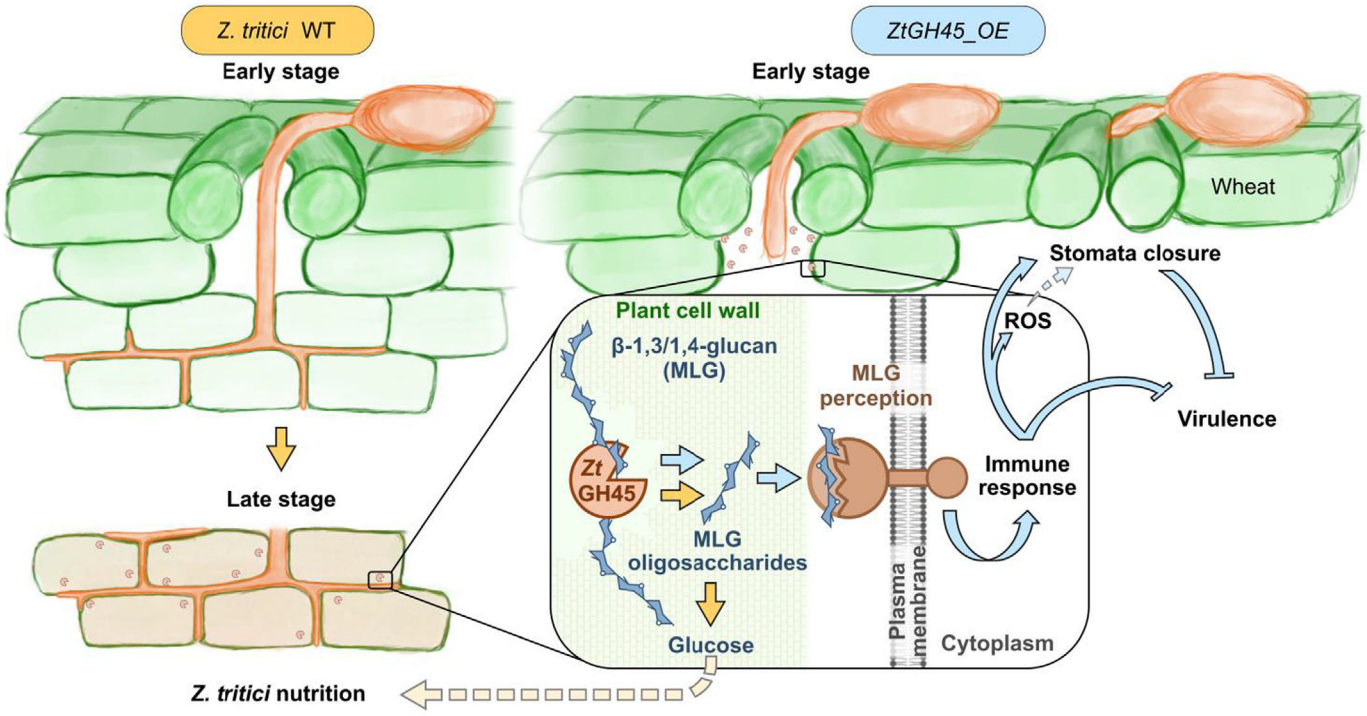

Fig. 5 Proposed model for the function of *Zt*GH45 during *Zymoseptoria tritici* infection of wheat plants. Mixed-linkage glucan (β-1,3/1,4-glucan; MLG) oligosaccharides are released during *Z. tritici* infection from wheat cell walls at the onset of the necrotrophic phase (yellow arrows, left side). By contrast, in plants inoculated with the line overexpressing *ZtGH45*, MLG-derived oligosaccharides are released earlier during infection, are perceived by wheat, and trigger an immune response, characterised by the induction of defence-related genes, production of reactive oxygen species, and stomatal closure, which hinders the progression of *Z. tritici* (blue arrows; right side). Dashed arrows indicate nonexperimentally proven information. ROS, reactive oxygen species; WT, wild-type; *ZtGH45_OE*, line overexpressing *ZtGH45*. Yellow and blue arrows indicate processes for *Z. tritici* WT and *Z. tritici_OE* respectively. Dashed arrows indicate hypotheses extracted from the results. Blunt-ended arrows indicate negative effects.

necrotrophic phase. However, disruption of *ZtGH45* does not impair virulence. We postulate that other proteins, including *Zt*GH12, might have redundant functions with *Zt*GH45 and be involved in nutrition, formation of pycnidia, or in triggering cell death. Alternatively, we cannot discard that *Zt*GH45-released oligosaccharides might be used to close the stomata once the pathogen is in the apoplast and, this way, keep high humidity conditions inside the host. Plant bacterial pathogens, when reaching the apoplast, release effectors that close the stomata to keep high humidity conditions (Melotto *et al.*, 2017).

Biotechnological strategies for crop protection based on the capacity of plant cell wall-derived oligosaccharides to increase plant resistance to pathogens have recently gained interest (Molina *et al.*, 2024a). Notably, pretreatment of plants with MLG oligosaccharides (especially MLG43) can protect different crops such as pepper, rice, and tomato against bacterial and fungal diseases (Rebaque *et al.*, 2021; Yang *et al.*, 2021). The ability to obtain these active oligosaccharides from plant-based industrial waste and plant biomass would contribute to the circular economy and enable more sustainable agriculture (Rebaque *et al.*, 2023). The results shown here illustrate the potential to apply this technology to wheat crops.

In conclusion, β-1,3/1,4-glucan oligosaccharides produced during *Z. tritici*-wheat interactions serve as danger signals triggering wheat immunity that leads to the production of ROS, stomatal closure, and a transcriptional response (Fig. 5). We propose that, over the course of evolution, the expression of the β-glucan-degrading enzyme *Zt*GH45, and probably other CAZymes, was limited to the necrotrophic stages when the pathogen has already colonised the apoplastic space, melanised pycnidia are being formed, and the MLG-triggered plant immune response may not effectively interfere with the pathogen progression.

Acknowledgements

This work was supported by grant PID2019-108693RA-I00, PID2023-150977NB-I00 and RYC2018-025530-I funded by MCIN/AEI/10.13039/501100011033 and European Social Funds (ESF) to ASV and grant PID2021-126006OB-I00 to AM, funded by MCIN/AEI/10.13039/501100011033 and by 'ERDF A way of making Europe,' and grant 'Severo Ochoa Program for Centres of Excellence in R&D (grant nos. SEV-2016-0672 and CEX2020-000999-S (2022–2025)) funded by MCIN/AEI/10.13039/501100011033 to AM. CCL and LM have been financially supported as postdoctoral researchers by CEX2020-000999-S (2022–2025) and CNS2023-144037 (funded by MICIU/AEI/10.13039/501100011033 and by EU NextGenerationEU/PRTR), respectively. DR was the recipient of an Industrial PhD fellowship and grant from the Madrid

Regional Government (IND2017/BIO-7800 to AM) and a 'Margarita Salas' postdoctoral fellowship European Union-NextGeneration EU UP2021-035 (RD 289/2021) from the Universidad Politécnica de Madrid. Work performed by HM was financed by PID2020-120364GA-I00 and PID2023-150378OB-I00 funded by MCIN/AEI/10.13039/501100011033. ALG was the recipient of a 'María Zambrano' postdoctoral fellowship/EU NextGenerationEU/PRTR from the Universidad de León. We thank Gero Steinberg and Sreedhar Kilaru (Exeter University, UK) for providing us with the 3D7-GFP line and Sara González Bodí (Bioinformatic Service Unit, CBGP) for providing us support with the bioinformatic analysis. We thank Cyrille Saintenac, Kostya Kanyuka, and Jean-Benoit Morel for providing us with wheat seeds.

Competing interests

None declared.

Author contributions

DR, CC-L, PK, AM, and AS-V designed the study. CC-L, DR, PK, GL, LM, FS, and SL-C performed the lab work. DR, CC-L, MJM, FV, and PK analysed the data and conducted statistical analyses. AL-G and HM performed, designed, and analysed HPAEC-PAD analysis. CL performed the synteny plot and the population analysis. BAM contributed to the design of the work, the selection, and functional characterisation of *Zt*GH45. DR, CC-L, and AS-V wrote the manuscript. All the authors critically reviewed and edited the manuscript.

ORCID

Cristian Carrasco-López https://orcid.org/0000-0001-5652-6595
Sergio López-Cobos https://orcid.org/0009-0005-1597-5083
Asier Largo-Gosens https://orcid.org/0000-0002-3415-9381
Cécile Lorrain https://orcid.org/0000-0001-9727-2616
Hugo Mélida https://orcid.org/0000-0003-1792-0113
María Jesús Martínez https://orcid.org/0000-0003-2166-1097
Bruce A. McDonald https://orcid.org/0000-0002-5332-2172
Lukas Meile https://orcid.org/0000-0002-2680-3309
Antonio Molina https://orcid.org/0000-0003-3137-7938
Diego Rebaque https://orcid.org/0000-0001-5343-7220
Andrea Sánchez-Vallet https://orcid.org/0000-0002-3668-9503
Felipe de Salas https://orcid.org/0000-0002-0057-0180
Francisco Vilaplana https://orcid.org/0000-0003-3572-7798

Data availability

We declare that the raw data is in the Dataset S1. The raw RNA-seq reads were deposited in the NCBI Sequence Read Archive (SRA) under the BioProject accession number PRJNA1276321.

References

Alassimone J, Praz C, Lorrain C, De Francesco A, Carrasco-López C, Faino L, Shen Z, Meile L, Sanchez Vallet A. 2024. The *Zymoseptoria tritici* avirulence factor AvrStb6 accumulates in hyphae close to stomata and triggers a wheat defense response hindering fungal penetration. *Molecular Plant Microbe Interactions* **37**: 432–444.

Aziz A, Gauthier A, Bézier A, Poinssot B, Joubert JM, Pugin A, Heyraud A, Baillieul F. 2007. Elicitor and resistance-inducing activities of beta-1,4 cellodextrins in grapevine, comparison with beta-1,3 glucans and alpha-1,4 oligogalacturonides. *Journal of Experimental Botany* **58**: 1463–1472.

Bacete L, Mélida H, Miedes E, Molina A. 2018. Plant cell wall-mediated immunity: cell wall changes trigger disease resistance responses. *The Plant Journal* **93**: 614–636.

Barghahn S, Arnal G, Jain N, Petutschnig E, Brumer H, Lipka V. 2021. Mixed linkage β-1,3/1,4-glucan oligosaccharides induce defense responses in *Hordeum vulgare* and *Arabidopsis thaliana*. *Frontiers in Plant Science* **12**: 682439.

Battache M, Lebrun M-H, Sakai K, Soudière O, Cambon F, Langin T, Saintenac C. 2022. Blocked at the stomatal gate, a key step of wheat Stb16q-mediated resistance to *Zymoseptoria tritici*. *Frontiers in Plant Science* **13**: 1–14.

Battache M, Suarez-Fernandez M, Klooster MV, Cambon F, Sánchez-Vallet A, Lebrun MH, Langin T, Saintenac C. 2024. Stomatal penetration: the cornerstone of plant resistance to the fungal pathogen *Zymoseptoria tritici*. *BMC Plant Biology* **24**: 736.

Bernasconi A, Lorrain C, Flury P, Alassimone J, McDonald BA, Sánchez-Vallet A. 2023. Virulent strains of *Zymoseptoria tritici* suppress the host immune response and facilitate the success of avirulent strains in mixed infections. *PLoS Pathogens* **19**: e1011767.

Bigeard J, Colcombet J, Hirt H. 2015. Signaling mechanisms in pattern-triggered immunity (PTI). *Molecular Plant* **8**: 521–539.

Boutrot F, Zipfel C. 2017. Function, discovery, and exploitation of plant pattern recognition receptors for broad-spectrum disease resistance. *Annual Review of Phytopathology* **55**: 257–286.

Bradley EL, Ökmen B, Doehlemann G, Henrissat B, Bradshaw RE, Mesarich CH. 2022. Secreted glycoside hydrolase proteins as effectors and invasion patterns of plant-associated fungi and oomycetes. *Frontiers in Plant Science* **13**: 853106.

Brandt B, Brodsky DE, Xue S, Negi J, Iba K, Kangasjärvi J, Ghassemian M, Stephan AB, Hu H, Schroeder JI. 2012. Reconstitution of abscisic acid activation of SLAC1 anion channel by CPK6 and OST1 kinases and branched ABI1 PP2C phosphatase action. *Proceedings of the National Academy of Sciences, USA* **109**: 10593–10598.

Bray NL, Pimentel H, Melsted P, Pachter L. 2016. Near-optimal probabilistic RNA-seq quantification. *Nature Biotechnology* **34**: 525–527.

Brunner PC, Torriani SFF, Croll D, Stukenbrock EH, McDonald BA. 2013. Coevolution and life cycle specialization of plant cell wall degrading enzymes in a hemibiotrophic pathogen. *Molecular Biology and Evolution* **30**: 1337–1347.

Cingolani P, Platts A, Wang LL, Coon M, Nguyen T, Wang L, Land SJ, Lu X, Ruden DM. 2012. A program for annotating and predicting the effects of single nucleotide polymorphisms, SnpEff. *Fly* **6**: 80–92.

Claverie J, Balacey S, Lemaître-Guillier C, Brulé D, Chiltz A, Granet L, Noirot E, Daire X, Darblade B, Héloir MC *et al.* 2018. The cell wall-derived xyloglucan is a new DAMP triggering plant immunity in *Vitis vinifera* and *Arabidopsis thaliana*. *Frontiers in Plant Science* **9**: 1725.

Costantini S, Benedetti M, Pontiggia D, Giovannoni M, Cervone F, Mattei B, De Lorenzo G. 2023. Berberine bridge enzyme–like oxidases of cellodextrins and mixed-linked β-glucans control seed coat formation. *Plant Physiology* **194**: 296–313.

Dai Y-S, Liu D, Guo W, Liu Z-X, Zhang X, Shi L-L, Zhou D-M, Wang L-N, Kang K, Wang F-Z *et al.* 2023. Poaceae-specific b-1,3;1,4-D-glucans link jasmonate signalling to OsLecRK1-mediated defence response during rice-brown planthopper interactions. *Plant Biotechnology Journal* **21**: 1286–1300.

Deller S, Hammond-Kosack KE, Rudd JJ. 2011. The complex interactions between host immunity and non-biotrophic fungal pathogens of wheat leaves. *Journal of Plant Physiology* **168**: 63–71.

Dobin A, Davis CA, Schlesinger F, Drenkow J, Zaleski C, Jha S, Batut P, Chaisson M, Gingeras TR. 2013. STAR: ultrafast universal RNA-seq aligner. *Bioinformatics* **29**: 15–21.

Drula E, Garron ML, Dogan S, Lombard V, Henrissat B, Terrapon N. 2022. The carbohydrate-active enzyme database: functions and literature. *Nucleic Acids Research* **50**: D571–D577.

Duncan KE, Howard RJ. 2000. Cytological analysis of wheat infection by the leaf blotch pathogen *Mycosphaerella graminicola*. *Mycological Research* **104**: 1074–1082.

Esquerré-Tugayé MT, Boudart G, Dumas B. 2000. Cell wall degrading enzymes, inhibitory proteins, and oligosaccharides participate in the molecular dialogue between plants and pathogens. *Plant Physiology and Biochemistry* **38**: 157–163.

Fernández-Calvo P, López G, Martín-Dacal M, Aitouguinane M, Carrasco-López C, González-Bodí S, Bacete L, Mélida H, Sánchez-Vallet A, Molina A. 2024. Leucine rich repeat-malectin receptor kinases IGP1/CORK1, IGP3 and IGP4 are required for arabidopsis immune responses triggered by β-1,4-D-Xylo-oligosaccharides from plant cell walls. *The Cell Surface* **11**: 100124.

Förster S, Schmidt LK, Kopic E, Anschütz U, Huang S, Schlücking K, Köster P, Waadt R, Larrieu A, Batistič O *et al.* 2019. Wounding-induced stomatal closure requires jasmonate-mediated activation of GORK K + channels by a Ca 2+ sensor-kinase CBL1-CIPK5 complex. *Developmental Cell* **48**: 87–99.

Francisco CS, Ma X, Zwyssig MM, McDonald BA, Palma-Guerrero J. 2019. Morphological changes in response to environmental stresses in the fungal plant pathogen *Zymoseptoria tritici*. *Scientific Reports* **9**: 9642.

Frandsen RJN, Andersson JA, Kristensen MB, Giese H. 2008. Efficient four fragment cloning for the construction of vectors for targeted gene replacement in filamentous fungi. *BMC Molecular Biology* **9**: 1–11.

Fry SC, Nesselrode BHWA, Miller JG, Mewburn BR. 2008. Mixed-linkage (1→3,1→4)-β-D-glucan is a major hemicellulose of *Equisetum* (horsetail) cell walls. *New Phytologist* **179**: 104–115.

Fuertes-Rabanal M, Rebaque D, Largo-Gosens A, Encina A, Mélida H. 2025. Cell walls: a comparative view of the composition of cell surfaces of plants, algae, and microorganisms. *Journal of Experimental Botany* **76**: 2614–2645.

Gámez-Arjona FM, Vitale S, Voxeur A, Dora S, Müller S, Sancho-Andrés G, Montesinos JC, Di Pietro A, Sánchez-Rodríguez C. 2022. Impairment of the cellulose degradation machinery enhances *Fusarium oxysporum* virulence but limits its reproductive fitness. *Science Advances* **8**: 9734.

Gao J, Huang JW, Li Q, Liu W, Ko TP, Zheng Y, Xiao X, Kuo CJ, Chen CC, Guo RT. 2017. Characterization and crystal structure of a thermostable glycoside hydrolase family 45 1,4-β-endoglucanase from *Thielavia terrestris*. *Enzyme and Microbial Technology* **99**: 32–37.

Geiger D, Scherzer S, Mumm P, Marten I, Ache P, Matschi S, Liese A, Wellmann C, Al-Rasheid KAS, Grill E *et al.* 2010. Guard cell anion channel SLAC1 is regulated by CDPK protein kinases with distinct Ca2+ affinities. *Proceedings of the National Academy of Sciences, USA* **107**: 8023–8028.

Gust AA, Pruitt R, Nürnberger T. 2017. Sensing danger: key to activating plant immunity. *Trends in Plant Science* **22**: 779–791.

Hahn MG, Darvill AG, Albersheim P. 1981. Host–pathogen interactions: XIX. The endogenous elicitor, a fragment of a plant cell wall polysaccharide that elicits phytoalexin accumulation in soybeans. *Plant Physiology* **68**: 1169.

Haueisen J, Stukenbrock EH. 2016. Life cycle specialization of filamentous pathogens – colonization and reproduction in plant tissues. *Current Opinion in Microbiology* **32**: 31–37.

Heckman KL, Pease LR. 2007. Gene splicing and mutagenesis by PCR-driven overlap extension. *Nature Protocols* **2**: 924–932.

Hsu PK, Dubeaux G, Takahashi Y, Schroeder JI. 2021. Signaling mechanisms in abscisic acid-mediated stomatal closure. *The Plant Journal* **105**: 307–321.

Kadowaki MAS, Polikarpov I. 2019. Structural insights into the hydrolysis pattern and molecular dynamics simulations of GH45 subfamily a endoglucanase from *Neurospora crassa* OR74A. *Biochimie* **165**: 275–284.

Kema GHJ, Yu D, Rijkenberg FHJ, Shaw MW, Baayen RP. 1996. Histology of the pathogenesis of *Mycosphaerella graminicola* in wheat. *Phytopathology* **86**: 777–786.

Keon J, Antoniw J, Carzaniga R, Deller S, Ward JL, Baker JM, Beale MH, Hammond-Kosack K, Rudd JJ. 2007. Transcriptional adaptation of *Mycosphaerella graminicola* to programmed cell death (PCD) of its susceptible wheat host. *Molecular Plant Microbe Interactions* **20**: 178–193.

Kong D, Hu HC, Okuma E, Lee Y, Lee HS, Munemasa S, Cho D, Ju C, Pedoeim L, Rodriguez B *et al.* 2016. L-Met activates Arabidopsis GLR Ca2+ channels upstream of ROS production and regulates stomatal movement. *Cell Reports* **17**: 2553–2561.

Krishnan P, Meile L, Plissonneau C, Ma X, Hartmann FE, Croll D, McDonald BA, Sánchez-Vallet A. 2018. Transposable element insertions shape gene regulation and melanin production in a fungal pathogen of wheat. *BMC Biology* **16**: 78.

Labavitch JM, Ray PM. 1978. Structure of hemicellulosic polysaccharides of *Avena sativa* coleoptile cell walls. *Phytochemistry* **17**: 933–937.

Lapalu N, Lamothe L, Petit Y, Genissel A, Delude C, Feurtey A, Abraham LN, Smith D, King R, Renwick A *et al.* 2023. Improved gene annotation of the fungal wheat pathogen *Zymoseptoria tritici* based on combined Iso-Seq and RNA-Seq evidence. *Molecular Plant Microbe Interactions*, (ja).

Lechner M, Findeiß S, Steiner L, Marz M, Stadler PF, Prohaska SJ. 2011. Proteinortho: detection of (Co-)orthologs in large-scale analysis. *BMC Bioinformatics* **12**: 1–9.

Liao Y, Smyth GK, Shi W. 2014. FEATURECOUNTS: an efficient general purpose program for assigning sequence reads to genomic features. *Bioinformatics* **30**: 923–930. Epub 2013 Nov 13.

Linde CC, Zhan J, McDonald BA. 2002. Population structure of *Mycosphaerella graminicola*: from lesions to continents. *Phytopathology* **92**: 946–955.

Liu Y, Maierhofer T, Rybak K, Sklenar J, Breakspear A, Johnston MG, Fliegmann J, Huang S, Roelfsema MRG, Felix G *et al.* 2019. Anion channel SLAH3 is a regulatory target of chitin receptor-associated kinase PBL27 in microbial stomatal closure. *eLife* **8**: 1–23.

Lorrain C, Feurtey A, Ller MM, Haueisen J, Stukenbrock E. 2021. Dynamics of transposable elements in recently diverged fungal pathogens: lineage-specific transposable element content and efficiency of genome defenses. *G3: Genes, Genomes, Genetics* **11**: jkab068.

Lorrain C, Zurich E, Feurtey A, Alassimone J, McDonald B. 2024. A novel genome-wide association approach reveals wheat pathogen genes involved in host specialization. *Research Square*. doi: 10.21203/rs.3.rs-4486034/v1.

Love MI, Huber W, Anders S. 2014. Moderated estimation of fold change and dispersion for RNA-seq data with DESEQ2. *Genome Biology* **15**: 1–21.

Martín-Dacal M, Fernández-Calvo P, Jiménez-Sandoval P, López G, Garrido-Arandía M, Rebaque D, del Hierro I, Berlanga DJ, Torres MÁ, Kumar V *et al.* 2023. Arabidopsis immune responses triggered by cellulose- and mixed-linked glucan-derived oligosaccharides require a group of leucine-rich repeat malectin receptor kinases. *The Plant Journal* **113**: 833–850.

Meile L, Carrasco-López C, Lorrain C, Kema GHJ, Saintenac C, Sánchez-Vallet A. 2025. The molecular dialogue between *Zymoseptoria tritici* and wheat. *Molecular Plant Microbe Interactions* **38**: 118–133.

Meile L, Croll D, Brunner PC, Plissonneau C, Hartmann FE, McDonald BA, Sánchez-Vallet A. 2018. A fungal avirulence factor encoded in a highly plastic genomic region triggers partial resistance to septoria tritici blotch. *New Phytologist* **219**: 1048–1061.

Meile L, Peter J, Puccetti G, Alassimone J, McDonald BA, Sánchez-Vallet A. 2020. Chromatin dynamics contribute to the spatiotemporal expression pattern of virulence genes in a fungal plant pathogen. *mBio* **11**: 1–18.

Mélida H, Bacete L, Ruprecht C, Rebaque D, Del Hierro I, López G, Brunner F, Pfrengle F, Molina A. 2020. Arabinoxylan-oligosaccharides act as damage associated molecular patterns in plants regulating disease resistance. *Frontiers in Plant Science* **11**: 1210.

Mélida H, Sopeña-Torres S, Bacete L, Garrido-Arandia M, Jordá L, López G, Muñoz-Barrios A, Pacios LF, Molina A. 2018. Non-branched β-1,3-glucan oligosaccharides trigger immune responses in Arabidopsis. *The Plant Journal* **93**: 34–49.

Melotto M, Zhang L, Oblessuc PR, He SY. 2017. Stomatal defense a decade later. *Plant Physiology* **174**: 561–571.

Molina A, Jordá L, Torres MÁ, Martín-Dacal M, Berlanga DJ, Fernández-Calvo P, Gómez-Rubio E, Martín-Santamaría S. 2024a. Plant cell wall-mediated disease resistance: current understanding and future perspectives. *Molecular Plant* **17**: 699–724.

Molina A, Sánchez-Vallet A, Jordá L, Carrasco-López C, Rodríguez-Herva JJ, López-Solanilla E. 2024b. Plant cell walls: source of carbohydrate-based signals in plant-pathogen interactions. *Current Opinion in Plant Biology* **82**: 102630.

Nakamura S, Mano S, Tanaka Y, Ohnishi M, Nakamori C, Araki M, Niwa T, Nishimura M, Kaminaki H, Nakagama T *et al.* 2010. Gateway binary vectors with the Bialaphos resistance gene, bar, as a selection marker for plant transformation. *Bioscience, Biotechnology, and Biochemistry* **74**: 1315–1319.

Palma-Guerrero J, Ma X, Torriani SFF, Zala M, Francisco CS, Hartmann FE, Croll D, McDonald BA. 2017. Comparative transcriptome analyses in *Zymoseptoria tritici* reveal significant differences in gene expression among strains during plant infection. *Molecular Plant Microbe Interactions* **30**: 231–244.

Plissonneau C, Hartmann FE, Croll D. 2018. Pangenome analyses of the wheat pathogen *Zymoseptoria tritici* reveal the structural basis of a highly plastic eukaryotic genome. *BMC Biology* **16**: 1–16.

Pring S, Kato H, Imano S, Camagna M, Tanaka A, Kimoto H, Chen P, Shrotri A, Kobayashi H, Fukuoka A *et al.* 2023. Induction of plant disease resistance by mixed oligosaccharide elicitors prepared from plant cell wall and crustacean shells. *Physiologia Plantarum* **175**: e14052.

Rebaque D. 2021. Novel cell wall-derived oligosaccharides trigger immune responses and disease resistance in plants.

Rebaque D, del Hierro I, López G, Bacete L, Vilaplana F, Dallabernardina P, Pfrengle F, Jordá L, Sánchez-Vallet A, Pérez R *et al.* 2021. Cell wall-derived mixed-linked β-1,3/1,4-glucans trigger immune responses and disease resistance in plants. *The Plant Journal* **106**: 601–615.

Rebaque D, López G, Sanz Y, Vilaplana F, Brunner F, Mélida H, Molina A. 2023. Subcritical water extraction of *Equisetum arvense* biomass withdraws cell wall fractions that trigger plant immune responses and disease resistance. *Plant Molecular Biology* **113**: 401–414.

Rudd JJ, Kanyuka K, Hassani-Pak K, Derbyshire M, Andongabo A, Devonshire J, Lysenko A, Saqi M, Desai NM, Powers SJ. 2015. Transcriptome and metabolite profiling of the infection cycle of *Zymoseptoria tritici* on wheat reveals a biphasic interaction with plant immunity involving differential pathogen chromosomal contributions and a variation on the hemibiotrophic lifest. *Plant Physiology* **167**: 1158–1185.

Sánchez-Vallet A, McDonald MC, Solomon PS, McDonald BA. 2015. Is *Zymoseptoria tritici* a hemibiotroph? *Fungal Genetics and Biology* **79**: 29–32.

Scherzer S, Maierhofer T, Al-Rasheid KAS, Geiger D, Hedrich R. 2012. Multiple calcium-dependent kinases modulate ABA-activated guard cell anion channels. *Molecular Plant* **5**: 1409–1412.

Schneider CA, Rasband WS, Eliceiri KW. 2012. NIH Image to ImageJ: 25 years of image analysis. *Nature Methods* **9**: 671–675.

Sørensen I, Pettolino FA, Wilson SM, Doblin MS, Johansen B, Bacic A, Willats WGT. 2008. Mixed-linkage (1 → 3),(1 → 4)-β-D-glucan is not unique to the Poales and is an abundant component of *Equisetum arvense* cell walls. *The Plant Journal* **54**: 510–521.

Steinberg G. 2015. Cell biology of *Zymoseptoria tritici*: pathogen cell organization and wheat infection. *Fungal Genetics and Biology* **79**: 17–23.

Stewart EL, Hagerty CH, Mikaberidze A, Mundt CC, Zhong Z, McDonald BA. 2016. An improved method for measuring quantitative resistance to the wheat pathogen *Zymoseptoria tritici* using high-throughput automated image analysis. *Phytopathology* **106**: 782–788.

Suarez-Fernandez M, Álvarez-Aragón R, Pastor-Mediavilla A, Maestre-Guillén A, del Olmo I, De Francesco A, Meile L, Sánchez-Vallet A. 2023. Sas3-mediated histone acetylation regulates effector gene activation in a fungal plant pathogen. *mBio* **14**: e0138623.

Torres MA, Dangl JL, Jones JDG. 2002. Arabidopsis gp91phox homologues Atrbohd and Atrbohf are required for accumulation of reactive oxygen intermediates in the plant defense response. *Proceedings of the National Academy of Sciences, USA* **99**: 517–522.

Vogel HJ. 1956. A convenient growth medium for Neurospora (medium N). *Microbial Genetics Bulletin* **13**: 42–43.

Voxeur A, Habrylo O, Guénin S, Miart F, Soulié M-C, Rihouey C, Pau-Roblot C, Domon J-M, Gutierrez L, Pelloux J. 2019. Oligogalacturonide production upon *Arabidopsis thaliana–Botrytis cinerea* interaction. *Proceedings of the National Academy of Sciences, USA* **116**: 19743–19752.

Wickham H. 2016. Data analysis. In: Springer-Verlag, ed. *ggplot2: elegant graphic design for data analysis*. New York, NY, USA; Cham, Switzerland: Springer, 189–201.

Yang C, Liu R, Pang J, Ren B, Zhou H, Wang G, Wang E, Liu J. 2021. Poaceae-specific cell wall-derived oligosaccharides activate plant immunity via OsCERK1 during *Magnaporthe oryzae* infection in rice. *Nature Communications* **12**: 1–13.

Zang H, Xie S, Zhu B, Yang X, Gu C, Hu B, Gao T, Chen Y, Gao X. 2019. Mannan oligosaccharides trigger multiple defence responses in rice and tobacco as a novel danger-associated molecular pattern. *Molecular Plant Pathology* **20**: 1079.

Zoghlami A, Paës G. 2019. Lignocellulosic biomass: understanding recalcitrance and predicting hydrolysis. *Frontiers in Chemistry* **7**: 874.

Zwiers LH, De Waard MA. 2001. Efficient *Agrobacterium tumefaciens*-mediated gene disruption in the phytopathogen *Mycosphaerella graminicola*. *Current Genetics* **39**: 388–393.

Supporting Information

Additional Supporting Information may be found online in the Supporting Information section at the end of the article.

Dataset S1 Raw data of the Figs 1–4, S2, S3, S5, S7–S9.

Fig. S1 Maps of plasmids used to obtain the overexpression and knockout mutants of *ZtGH45* and validation of the obtained *Zymoseptoria tritici* transformant lines.

Fig. S2 Characterisation of β-glucan oligosaccharides released during *Zymoseptoria tritici*–wheat infection.

Fig. S3 Expression pattern of *Zymoseptoria tritici* genes encoding for CAZymes with putative β-1,4-glucanase activity (EC 3.2.1.4).

Fig. S4 *Zymoseptoria tritici Zt*GH45 harbours a conserved catalytic domain.

Fig. S5 Early expression of active *ZtGH45* impairs virulence and reproduction of *Zymoseptoria tritici* in wheat.

Fig. S6 Overexpression of *ZtGH45* in *Zymoseptoria tritici* does not affect growth and stress tolerance.

Fig. S7 The catalytic site of *Zt*GH45 is required to induce resistance in wheat.

Fig. S8 Lines of *Zymoseptoria tritici* that overexpress *ZtGH45* degrade β-glucan polysaccharides.

Fig. S9 Wheat response upon MLG43 and cellotriose treatment.

Table S1 *ZtGH45* annotations in different *Zymoseptoria tritici* strains.

Table S2 Primers used in this work.

Table S3 Summary of the wheat and *Zymoseptoria tritici* transcriptomic dataset.

Table S4 Fold change (Log_2) expression levels of wheat genes upon MLG43, or cellotriose (Cello3) treatment (3h) compared to mock or upon infection with *Zymoseptoria tritici* 3D7 or *ZtGH45_OE*-infected plants compared to mock treated plants (6 dpi).

Table S5 Counts and CPMs of wheat genes upon MLG43, or cellotriose (Cello3) treatment (3h) or upon infection with *Zymoseptoria tritici* 3D7 or *ZtGH45_OE* lines (6 dpi).

Table S6 Gene ontology (GO) analysis of upregulated wheat genes in response to MLG43.

Table S7 Upregulated wheat genes in response to MLG43. Genes potentially involved in defence are highlighted in green.

Table S8 Wheat genes specifically upregulated in *ZtGH45_OE*-infected plants and not upregulated in 3D7-infected plants. Fold change (Log_2) of the expression in plants infected with *ZtGH45_OE* compared to the control is shown. Genes potentially involved in defence are highlighted in green.

Table S9 Gene ontology (GO) analysis of wheat genes specifically upregulated in *ZtGH45_OE*-infected plants and not upregulated in 3D7-infected plants.

Table S10 Counts and normalised values of the expression of *Zymoseptoria tritici* genes in the wild-type and *ZtGH45_OE* lines.

Table S11 Differentially expressed *Zymoseptoria tritici* genes in *ZtGH45_OE*-infected plants with respect to 3D7-infected plants. Fold changes (Log_2) of *ZtGH45_OE* compared to 3D7 at 6 d post infection (dpi) are indicated.

Table S12 Genes upregulated in wheat upon infection with *Zymoseptoria tritici Zt*GH45-overexpression line (ZtGH45_OE; 6 d post infection), but not with the wild-type strain, and upon treatment with 0.5 mM MLG43 (3 h after treatment), but not with 0.5 mM Cello3.

Please note: Wiley is not responsible for the content or functionality of any Supporting Information supplied by the authors. Any queries (other than missing material) should be directed to the *New Phytologist* Central Office.